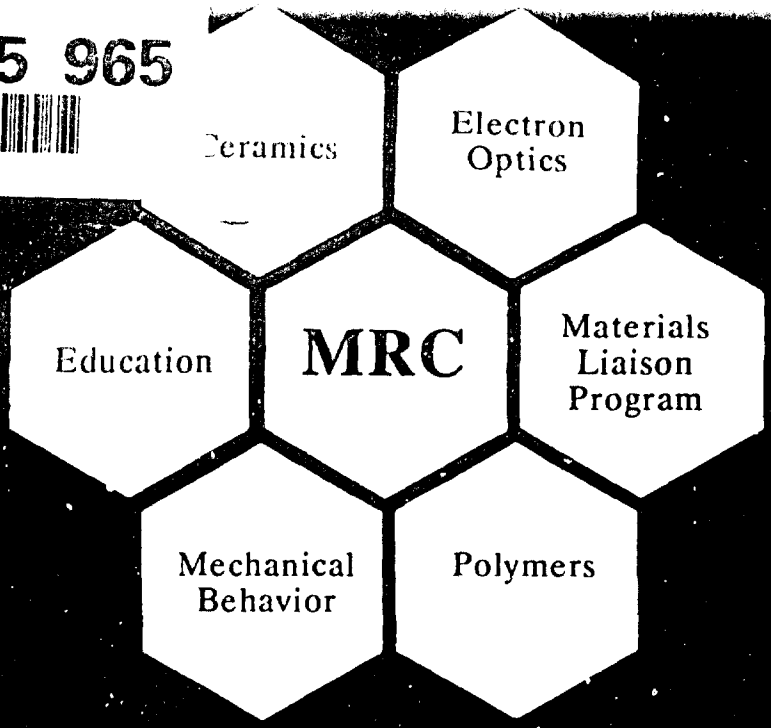

SECOND ANNUAL REPORT

PROCESSING OF NOVEL NANOPARTICLE DISPERSION STRENGTHENED CERAMICS FOR IMPROVED MECHANICAL PERFORMANCE

Professors H. M. Chan, (P.I.), M. P. Harmer (Co-P.I.),
and Research Assistants/Associates
M. Thompson, J. Fang, I. Chou

Sponsored by

U.S. Office of Naval Research and
The Electric Power Research Institute

ONR Grant No.: N00014-92-J-1635 Mod. P00002

EPRI Contract: RP2426-54 Amend. 1

Report Period: 15 December 1992 - 14 December 1993

Materials Research Center, MRC
Lehigh University

ABSTRACT

Results from a previous study carried out by the Lehigh group demonstrated that Al_2O_3:SiC nanocomposites exhibited superior mechanical behavior relative to single phase alumina only when the samples had been annealed (2 h at 1300 °C in argon) subsequent to industrial machining. These results were rationalized by postulating that on annealing of the machined specimens:-

a) The extent of healing of grinding induced flaws is more significant in the nanocomposite than in alumina.

b) The machining induced residual stresses are relaxed to a lesser degree in the nanocomposite than in alumina.

Further model studies have now been carried out which provide definitive evidence that both of the above assumptions are correct. Observation of indentation induced cracks both prior to, and after annealing, revealed that in the nanocomposite cracking is predominantly transgranular, and *crack healing* takes place on annealing. For the case of single phase alumina, however, the crack morphology is predominantly intergranular, and annealing causes *crack growth.*

In addition, experiments were undertaken whereby small "satellite" indents were used to probe the stress field distribution around a larger central indentation. Due to the influence of the radial compressive, and circumferential tensile stresses around the large indentation, the radial cracking at the small indents was highly asymmetrical. However, if the large indents are introduced prior to annealing, and the "satellite" indents only made after annealing, it was observed that in the case of alumina, the radial crack pattern at the small indents was now symmetrical. In contrast, the radial crack morphology for the nanocomposite still exhibited significant asymmetry, thus proving that relaxation of residual stresses occurs more readily in the single phase material compared to the nanocomposite.

Preliminary TEM observations of the dislocation structures in machined/annealed specimens revealed markedly different results for the two types of material. In alumina, substantial recovery had taken place giving rise to a fine subgrain structure. For the nanocomposite, however, the retained dislocation density was very high, and there was evidence of dislocation pinning by extremely fine ($\sim$ 10 nm) SiC particles.

In order to monitor the extent of machining induced stresses (and their subsequent relaxation) in a more quantitative manner, the capability to carry out laser-interferometry has been established at Lehigh. This technique enables the measurement of specimen curvature of thin disks, from which the magnitude of macroscopic residual stresses may be readily derived.

In addition, tensile creep testing of nanocomposite specimens is now underway. Preliminary results indicate that the creep rate of the nanocomposite is significantly lower than that of alumina.

In the forthcoming grant period the aim will be to establish the materials/processing parameters required for nanocomposites to achieve optimum mechanical properties. Given a fundamental understanding of the strengthening mechanisms in nanocomposite materials, it should be relatively straightforward to extend such principles to other ceramic systems.

TABLE OF CONTENTS

Section 1.1

CRACK HEALING AND STRESS RELAXATION IN Al_2O_3-SiC "NANOCOMPOSITES"

by

A. Mark Thompson, Helen M. Chan, and Martin P. Harmer

Submitted to Journal of the American Ceramic Society

Crack Healing and Stress Relaxation in Al_2O_3-SiC "Nanocomposites"

A. Mark Thompson*, Helen M. Chan* and Martin P. Harmer*
Dept of Materials Science & Engineering, and Materials Research Center,
Lehigh University,
Bethlehem, PA 18015

Robert F. Cook*
IBM Research Division,
T. J. Watson Research Center,
Yorktown Heights, NY 10598

The crack healing behavior of Al_2O_3 and Al_2O_3-SiC nanocomposite was studied using Vickers indentations to generate precracks. Cracks were characterized using both optical and scanning electron microscopy. After annealing in argon for 2 h at 1300 °C, radial cracks in the nanocomposite healed: The cracks closed and there was a small degree of re-bonding in the vicinity of the crack tip. In contrast, radial cracks in alumina grew when exposed to the same annealing treatment. The different responses are attributed to the fracture mode and toughening mechanism in each material: In the nanocomposite, the cracks close as the residual stresses surrounding the indentations relax. Radial cracks open and grow in alumina because microstructural toughening is diminished during heating to the annealing temperature. An implication is that strength-limiting machining flaws in these materials behave similarly, thereby accounting for the strengthening effect of annealing in this "nanocomposite" system.
(Key Words: alumina, silicon carbide, nanocomposite, crack healing, indentation.)

* Member ACerS

I. Introduction

The mechanical properties of single-phase ceramics can be improved significantly by the addition of sub-micron reinforcing particles. For example, recent works by Niihara et al.[1-4] reported that as little as 5 vol% of 0.3 μm SiC particles could increase the strength of hot-pressed Al_2O_3 from 350 MPa to over 1 GPa. Annealing further enhanced the strength of this "nanocomposite" to 1.5 GPa. In addition to these high strengths, it was reported that the toughness of the alumina was improved from 3.25 MPa $m^{1/2}$ to 4.7 MPa $m^{1/2}$ with the SiC additions. Proposed toughening mechanisms included crack deflection, and microcracking induced by thermal expansion mismatch between the particles and matrix grains. The beneficial strengthening effect of the annealing was attributed to a reduction in the dominant flaw size, possibly through the refinement of matrix grains by dislocation interaction, the healing of surface cracks, or the prevention of grain-boundary fracture during cooling.

Subsequent work by Zhao et al.[5,6] confirmed the strengthening of alumina by SiC additions. In their work, annealing for 2 hours at 1300 °C increased the intrinsic strength of the nanocomposite from 700 MPa to approximately 1 GPa. In contrast to Niihara's work, they found that the toughness increase was modest and not sufficient to account for the vast improvement in strength. Instead, they proposed that the strengthening and apparent toughening arose from machining-induced compressive surface stresses. Their results and hypothesis are summarized in Fig. 1. It was suggested that, during grinding of the test specimens, compressive stresses and machining flaws were introduced into the specimen surfaces. These compressive surface stresses increased the apparent toughness of the nanocomposite, as determined by indentation-strength tests. On annealing, the residual surface stresses were relaxed slightly by diffusional processes. Consequently, the apparent toughness of the nanocomposite decreased and the indentation-strength curve was displaced to lower strengths. The *intrinsic* strengths of unindented specimens reflected both the apparent toughness and the size of the dominant (machining) flaws. Flaw healing during annealing more than compensated for the relaxation of the surface compressive stresses, and the unindented strengths were thus improved significantly. In the case of single-phase alumina, it was proposed that the residual surface stresses relaxed completely on annealing, again leading to a reduction in apparent toughness. However, in contrast to the nanocomposite,

the crack healing accompanying this stress relaxation was not sufficient to improve the intrinsic strength. Central to the hypothesis of Zhao et al. is the assumption that the stress relaxation and crack-healing behavior of the materials were dissimilar, i.e., cracks were able to heal more easily in the nanocomposite. If true, an implication is that microstructures can be developed that are amenable to strengthening by crack healing.

The importance of crack healing as a strengthening mechanism in ceramics has prompted numerous studies.[7-34] Cracks and flaws have been introduced by a variety of means including mechanical contact (inscribing,[7] impacting,[8] machining[9-11] or indenting[12-17]), thermal shock,[18-27] and more recently, lithographic techniques.[28-31] Although the initial flaw size and stress state in each of these cases was distinct, the healing behavior was governed by the same energy balance criterion: There is a driving force to close a crack when the mechanical energy release rate, G, falls below twice the surface free energy per unit area, 2γ, i.e., $G < 2\gamma$.[35-37] When a crack is not subject to applied or residual stresses (i.e., $G \rightarrow 0$) the inequality clearly holds and the driving force for healing is the reduction in total surface free energy.

In the absence of chemical reactions, there are two dominant crack-healing mechanisms; (i) adhesion,[8,12,27,33,36-39] and (ii) diffusional bonding.[7,14,15,18-21,23-26,28-32] Adhesion describes the process of atomic rebonding across the interface as the fracture surfaces mate. The rate at which the crack heals depends on the kinetics of atomic rebonding and the magnitude of the deviation from equilibrium (G - 2γ).[35] Note that although healing by adhesion requires no long-range diffusion of atoms along the fracture surfaces, crack healing can also be limited by the rate at which adsorbed species are expelled from the retracting crack tip.[36,37]

Diffusional bonding is driven by variations in local surface curvature and requires long-range surface rearrangement of material. This process has been described[20] as a series of geometrically distinct stages: During the initial stage, the crack tip blunts and recedes. The amount of recession is dependent on the crack geometry, crack face and crack edge orientation, sample chemistry,[30,31] and the method by which the crack was introduced.[20] For example, cracks created by mechanical techniques showed a greater degree of recession than stress-free flaws (introduced by thermal shock or lithographic techniques). The onset of the intermediate stage is characterized by discontinuous joining (or pinching) of the crack surfaces behind the blunt tip via Rayleigh instabilities.[40] Further instabilities generate cylindrical pores which in turn either

spheroidize or ovulate to develop arrays of isolated pores, as modeled by Nichols and Mullins.[41-44] The final stage of crack healing is analogous to the final stage of sintering in which isolated pores shrink.

The relative importance of each of these mechanisms to a crack healing event is governed by their relative kinetics and, consequently, by the conditions under which the crack is healing. At low or intermediate temperatures, when surface diffusion is minimal, adhesion is the dominant crack healing mechanism. For example, there is evidence of partial microcrack healing in alumina even at room temperature.[27] Diffusional bonding becomes important in alumina at temperatures approaching the sintering temperature, as shown by the break-up of lithographically -introduced pores in sapphire at 1800 °C.[28-31] It is unclear which of these two mechanisms was dominant at the annealing temperature used to strengthen the nanocomposites.

The purpose of the following work was to characterize the crack healing and stress relaxation behavior of Al_2O_3, and Al_2O_3 containing 5 vol% 0.15 μm SiC particles under the annealing conditions that gave rise to the vast strength increases in the nanocomposite. Because machining flaws are difficult to observe, the initial flaws were introduced via Vickers indentation. The indentation technique develops controlled flaws and can, therefore, act as a probe to compare the crack healing behavior of the two materials. From a practical point of view, this technique should also simulate the impact damage that can be expected when the ceramic is in service.

II. Background Theory

When a sharp indenter is loaded onto a brittle material, above a critical load, radial cracks emanate from the impression perpendicular to the surface. On unloading, and sometimes during loading, these radial cracks grow under the residual tensile stress field.[45-47] The cracks arrest when the stress-intensity factor arising from this residual stress field is counterbalanced by the intrinsic material toughness such that

$$K_r\,(c_o) = T_o \qquad (1)$$

where $K_r(c_o)$ is the residual stress-intensity factor, T_o is the intrinsic material toughness in the testing environment, and c_o is the arrested equilibrium crack length. When the material exhibits microstructural toughening (*R*-curve behavior), the equilibrium condition is modified to

$$K_r(c_o) = T_o + T_\mu(c_o) \tag{2}$$

where $T_\mu(c_o)$ represents the microstructural toughening component and is also a function of the crack length.

The residual stress-intensity factor most commonly assumed for indentation half-penny and radial cracks is[45]

$$K_r = \frac{\chi_r P}{c^{3/2}} \tag{3}$$

where c is the crack length, P is the peak indention load, and χ_r is the residual stress parameter, a dimensionless coefficient that reflects the magnitude of the residual elastic-plastic contact deformation field.[45] The residual stress parameter is in turn given by

$$\chi_r = \xi\left(\frac{E}{H}\right)^{1/2} \tag{4a}$$

where E is the Young's modulus, $H = P/2a^2$ is the hardness, and ξ is a material-independent calibration constant.[46] It is important to note that Eq. 4(a) is only valid in the immediate post-indentation configuration. It is derived from the more general proportionality

$$\chi_r \propto \left(\frac{a}{b}\right)\left(\frac{E}{H}\right) \tag{4b}$$

where a^3 is a measure of the volume of material displaced by the indentor, and b^3 is a measure of the volume of the plastic zone accommodating the displaced material.[45] The magnitudes of a and b may vary from their post-indentation values on aging or annealing, thereby altering χ_r. E and H are fixed at their values under the indentation conditions.

Combining Eqs. (1) through (3) yields general expressions for the equilibrium indentation

crack length

$$c_e = \left(\frac{\chi_r P}{T_o}\right)^{2/3} \tag{5a}$$

when material does not exhibit *R*-curve behavior, and

$$c_e = \left(\frac{\chi_r P}{T_o + T_\mu(c_e)}\right)^{2/3} \tag{5b}$$

when there is a microstructural toughening component.

The possible influences of annealing on the equilibrium crack length can now be considered. For a given indentation load, P, the crack length will be governed by the ratio of χ_r to the overall material toughness, $T = T_o + T_\mu$. During annealing, the residual stresses relax, effectively reducing χ_r through a decrease in the ratio (a/b) in Eq. 4(b). Physically, this decrease may occur either by an expansion of the plastic deformation zone, or contraction of the remnant impression. For example, during the annealing of metals, dislocations migrate away from the indentation site, effectively enlarging the plastic zone. The converse is true for polymers: On annealing, macroscopic flow reduces the impression volume. In ceramics, the physical picture of stress relaxation is less clear because several mechanisms may operate simultaneously. For example, diffusional re-arrangement of material within the plastic deformation zone may be accompanied by lateral crack growth outside the zone. While the former could be described as a reduction in the impression volume, the latter has been modeled by an enlargement of the plastic zone.[48] Regardless of the mechanism, the thermal activation of annealing permits a reduction in the residual strain energy, which results in a decrease in χ_r.

For the simplest case in which there is no microstructural toughening, the crack length is governed by the ratio (χ_r/T_o). If the intrinsic toughness remains constant or increases on annealing then (χ_r/T_o) diminishes and the crack should close.[35] If, on the other hand, the intrinsic toughness decreases, there are two possible scenarios: When the stress-relaxation rate exceeds the rate at which the toughness decreases, (χ_r/T_o) is reduced and there will be a driving force to

close the crack. Conversely, when the intrinsic material toughness decreases more rapidly than the residual stresses, the crack should propagate. Note, however, that in the latter case the crack should ultimately heal as the residual stresses will eventually relax completely.

This approach can be extended to include materials in which there is a microstructural toughening component. In this case, the equilibrium crack length depends on the relative change in the ratio $\chi_r/(T_o + T_\mu)$. The crack should close if the overall material toughness $(T_o + T_\mu)$ remains constant or increases during annealing. When there is a reduction in either the intrinsic material toughness or the miscrostructural toughening, then the relative kinetics must again be considered. If $(T_o + T_\mu)$ decreases more rapidly than the rate at which χ_r diminishes, the crack should grow. This case is especially important for non-cubic materials, in which the microstructural toughening is believed to be temperature-dependent,[49-51] a point that will be readdressed in the discussion.

III. Experimental Procedure

Experiments were conducted using the hot-pressed, mechanical testing bars fabricated by Zhao et al.[6] Two materials were studied: undoped Al_2O_3, and Al_2O_3 containing 5 vol% 0.15 μm SiC particles. All samples had been annealed previously in argon for 2 hours at 1300 °C, indented and then tested in four point bending. In order to remove the silicone oil remaining from the mechanical testing procedure, the polished surfaces of the bars were lightly polished with a 0.3 μm alumina slurry. The samples were then washed in acid (aqua regia followed by HF) to remove further surface contamination.

The cleaned samples were re-indented using a Vickers diamond pyramid with peak contact loads ranging from 10 N-100 N. Each bar was indented at numerous points along its length with sufficient space between indentations to avoid interaction of the stress fields surrounding the impressions. Three bars of each material were indented. Crack lengths were measured in air immediately after indenting using a scattered darkfield optical technique.[52] The same cracks were re-measured on all samples immediately prior to annealing. The bars were placed in a covered alumina crucible and annealed in argon for 2 hours at 1300 °C in a graphite-lined furnace. The atmosphere inside the furnace was sufficiently reducing to prevent significant oxidation of the

SiC particles. Immediately after annealing the crack lengths were remeasured.

One bar of each material was subjected to the experimental procedure outlined in Fig. 2. Prior to the optical crack length measurements, the bar was clamped in a jig and imaged uncoated using 3.1 kV accelerating voltage in a scanning electron microscope (SEM). Immediately after annealing, the crack lengths were remeasured and the bar was re-imaged uncoated in the SEM. The elapsed time between the initial and final SEM observations in each case was less than 24 h. Because this elapsed time was negligible compared to the time between indentation and annealing (>300 h.) it is assumed that the SEM observations represented the crack configuration immediately prior to and immediately after annealing.

IV. Results

(A) Optical Observation of Radial Cracks

The indentation crack lengths in both the Al_2O_3 and composite appeared to be insensitive to the moisture in the laboratory atmosphere. Table I gives the crack lengths measured from a single specimen immediately after indenting and immediately prior to annealing (each value represents the mean and standard deviation of at least 12 crack lengths). There was no significant increase in crack length in either material even though the samples had been left under normal laboratory conditions in excess of 300 hours. Therefore, it appears that there was relatively little sub-critical crack growth after indentation in these materials.[35,46] Accordingly, it can be assumed that the crack length measured immediately prior to annealing represented the crack size obtained after indentation.

A typical indentation in the nanocomposite is shown in the optical micrograph of Fig. 3(A). Straight cracks emanate from the four corners of the impression, consistent with the classical description of the radial crack system.[45-47] The arrows in Fig. 3(A) mark the furthest points at which the cracks could be resolved. On annealing, these cracks appeared to heal: The original crack tip could not be located and the arrows in Fig. 3(B) mark the tips of the annealed cracks. The semi-diagonals and crack lengths measured from multiple indentations on at least three specimens are shown in Fig. 4(A). The indentation semi-diagonal, a, was consistent with a $P^{1/2}$-dependence, indicating that the hardness in each material was constant over the indentation

range studied. Annealing did not significantly affect the indentation diagonal. In accordance with Eq. 5(a), the crack length, c_0, measured prior to annealing was consistent with a $P^{2/3}$-dependence. This dependency indicates that the toughness was constant over the indentation range studied, and that there was little change in the interaction of lateral cracks and the radial cracks.[53] After annealing, the crack lengths were significantly shorter. For example, at the 10 N indentation load, a 50 μm crack appeared to heal on average by approximately 20 μm.

Corresponding optical micrographs for alumina are shown in Figs. 3(C) and (D). As the relative density of this alumina was 99.5%,[6] the voids observed on the polished surface are believed to be the result of grain pull-out during the original industrial polishing. The four radial cracks emanating from the corners of the impression seemed to interact with the microstructure and were not as straight as those in the nanocomposite. After annealing, no appreciable healing of these cracks was observed (see Fig. 3(D)). Instead, the cracks became more distinct: The surface traces were more clear and the occasional crack even appeared to propagate slightly, as indicated by point P in Figs. 3(C) and (D). The variation in crack length was not sufficient to significantly alter the average crack length measurements, as detailed in Table I and Fig. 4(B).

In summary, the optical observations indicated that the healing behavior of indentation cracks in the nanocomposite and alumina were different: The cracks in the composite healed, whereas those in alumina remained open.

(B) SEM Observation of Radial Cracks

The polished surface of the composite material is shown in its as-indented condition in Fig. 5(A). It can be seen that the SiC particles were well dispersed and typically isolated as individual sub-micron particles. Occasional SiC agglomerates were observed. The crack shown emanated from a 10-N indentation, and was characteristic of indentation cracks in this material; the fracture path was quite flat and predominantly transgranular. These observations are consistent with previous work in this composite system.[1-6] The crack is visibly open along the majority of its length and the tip appears to arrest inside one of the alumina grains, as indicated.

On annealing, the crack opening displacement decreased to the extent that the opposing fracture surfaces mated (see Fig. 5(B)). Along the original crack plane a trail can still be seen, which indicates that the fracture surfaces did not bond completely. Only the region nearest the

crack tip has disappeared, and presumably bonded. Note that the scale of this "true" healing is only on the order of a 1-2 μm. This is in contrast to the optical crack length measurements which indicated that a 10-N indentation crack healed by approximately 20 μm.

The polished surface of an Al_2O_3 sample is shown in Fig. 6, both in the (A) as-indented and (B) annealed states. The crack shown emanated from a 50-N impression. In this case, the fracture path was more tortuous than that in the composite and was predominantly intergranular, arresting along the grain boundary indicated. On annealing, the crack did not close but actually grew; the opening displacement increased and the crack penetrated further along grain boundaries (see Fig. 6(B)). The extent of this crack growth was only on the order of 5 μm, which was too small to be identified from the optical measurements.

The observations of Figs. 5(A) and (B), and 6(A) and (B) are summarized in the crack opening displacement (COD) measurements of Figs. 5(C) and 6(C), respectively. (The opening displacements were measured normal to the long axes of the images using a digital imaging technique.) Note that the abscissa is scaled to match the magnification of the images, whereas the ordinates have been expanded for clarity. The fine dashed lines represent the as-indented COD and the bold solid lines represent the COD after annealing.

The SEM observations confirmed the healing of radial cracks in the composite; however, the extent of "true" crack healing was much smaller than that indicated in the optical observations. In addition, the high magnification images revealed that the radial cracks in alumina propagated, a phenomenon that was not identifiable using optical techniques.

V. Discussion

An important assumption in the hypothesis of Zhao et al.[6] was that flaw healing in the nanocomposite and alumina were dissimilar. Specifically, they believed that machining flaws in the nanocomposite healed sufficiently during annealing to generate large intrinsic strengths, whereas similar flaws in the alumina did not. The current work supports this assumption: Indentation radial cracks in the nanocomposite healed, whereas those in the alumina grew. (Indentation flaws are similar to dominant, strength-limiting machining flaws in that the cracks extend beyond compressive plastic deformation zones.) As a consequence of this difference in

healing behavior, the annealing step has a more beneficial effect on the composite than on the alumina, consistent with the intrinsic strengths measured in previous work.[6]

The experimental observations are indicative of crack healing by an adhesive, rather than by a diffusive mechanism: Crack tip morphology was not altered significantly,[20] and pinch-off and isolated pores were not observed, in spite of the substantial decreases in COD in the composite. Moreover, diffusive healing mechanisms are inconsistent with the crack extension observed in the alumina. A previous indentation crack-healing study also concluded that adhesion was the dominant crack-healing mechanism at similar temperatures to those used here.[12] The healing behavior is therefore more properly studied as a fracture process, driven by stress fields, rather than as a sintering-related process, driven by variations in local surface curvature. The different response of the two materials is thus explained by considering their fracture modes and toughening mechanisms.

The toughness of many polycrystalline alumina materials increases as cracks extend (*R*-curve behavior).[54,55] The principal mechanism for this increasing fracture resistance is grain-localized bridging behind a crack tip that propagates intergranularly.[55-57] Energy is dissipated pulling out interlocking grains against the constraint of frictional tractions that are attributed to the thermal expansion anisotropy.[51] (As alumina cools from its fabrication temperature, thermal expansion anisotropy generates stresses between adjacent grains.[49]) If the fracture path is flat and transgranular, grain bridging is minimal and such microstructural toughening is not realized.

Fracture in the nanocomposite was predominantly transgranular. Therefore, it can be assumed that toughening by microstructural bridging was absent (i.e. $T = T_o$) in which case the equilibrium crack lengths are given by Eq. 5(a). After annealing, the radial cracks closed, indicating that the ratio (χ_r/T_o) was reduced. (It may be speculated that the radial cracks may have propagated prior to closing; however there was no surface trace to indicate this extension.) Closing of the cracks would be expected if (i) the intrinsic material toughness increased (or remained constant), or if (ii) the residual stress relaxation rate exceeded the rate at which the intrinsic material toughness diminished. The effect of annealing on the intrinsic toughness of the nanocomposite cannot be determined from these observations. However, previous work has shown that the toughness of sapphire decreases with increasing temperature.[58,59] If this is the

case, then the reduction in toughness occurs too slowly to prevent closing of the predominantly transgranular radial cracks.

The proposed flaw healing behavior of the nanocomposite is described schematically in Fig. 7. The equilibrium crack length obtained after indenting remained unchanged during heating to the annealing temperature (see Fig. 7(A)). Subsequent relaxation of the residual stress field during annealing reduced the stress-intensity factor, K_r, wedging open the crack. As a consequence the crack closed (see Fig. 7(B)). At this point, it is important to note that the closing of the crack depends not only on the kinetics of the healing mechanism but also on the mode of the original fracture: Surface asperities can obstruct the mating of the fracture surfaces. In the case of the nanocomposite, the fracture mode was conducive to healing: The fracture path was relatively flat with few asperities. In addition, the fracture path was predominantly transgranular. Therefore, grains on opposing crack faces had the same orientation and, consequently, the same coefficients of thermal expansion. Frictional tractions at asperities would, therefore, have been minimized.

In contrast to the nanocomposite, the fracture path of the radial cracks in the alumina was predominantly intergranular, and therefore the microstructural toughening component, T_μ, cannot be ignored. In this case the equilibrium crack lengths are governed by Eq. 5(b). The growth of the radial cracks indicates that the ratio $\chi_r/(T_o + T_\mu)$ increased on annealing. If the intrinsic material toughness, T_o, remained constant, then an increase in this ratio would require *both* that the microstructural toughening decrease, and that it decrease faster than the residual stress field relaxes. On heating to the annealing temperature, the stresses associated with the thermal expansion anisotropy of alumina diminish, thereby, reducing the frictional tractions that give rise to microstructural toughening. The net toughness therefore decreases, consistent with other observations in polycrystalline alumina.[60] Note that the rate at which the toughness diminishes is then dependent solely on the heating rate. In contrast the relaxation of the residual contact stress field surrounding the impression decays at a rate governed by diffusional processes. Thus it is proposed that the radial cracks grow because the microstructural toughening decays more rapidly than the residual stress field driving force.

This proposed mechanism of crack growth in alumina is explained schematically in Fig.

8. After indentation, the radial crack propagated until the residual stress-intensity factor was balanced by the material's intrinsic toughness and the frictional tractions between adjacent grains (microstructural toughening). These frictional tractions are depicted in Fig. 5(A) as a stress, σ_f, acting normal to the grain boundaries. During heating to the annealing temperature, the thermal expansion mismatches decreased, thereby, reducing the magnitude of the frictional tractions. As this decreased the overall material toughness, the radial crack extended (see Fig. 5(B)). Subsequent relaxation of the residual stress field surrounding the impression reduced the driving force wedging open the radial crack (see Fig. 5(C)). Under these circumstances, the crack should have healed. However, it remained open for two reasons: First, the fracture path in the alumina was tortuous. It may be difficult to mate two opposing surfaces with such a rough topography. Second, the frictional tractions may not have disappeared completely at the annealing temperature (see Fig. 5(C)). The same frictional tractions that opposed further crack growth at this temperature would have prevented surface asperities from sliding past each other. For example, one could envision frictional tractions at the grain facet, F, indicated in Fig. 6(B). Closing the crack would, therefore, have required an additional driving force to act against these remaining frictional tractions.

It is proposed that radial cracks initially propagate in alumina because the microstructural toughening decays more rapidly than the residual stress field relaxes. Once the residual stress field relaxes, the cracks are prevented from closing because of the tortuous fracture path and the remnant thermal expansion anisotropy. In principle, this crack opening phenomenon should be more pronounced in coarse-grained alumina, which exhibits much stronger *R*-curve behavior.[51,54-57] However, indentations in coarse-grained alumina are typically non-ideal:[46,47,53] They are susceptible to artefacts such as chipping, lateral cracking, and the generation of more than four radial cracks. Each of these complicates this simple description of crack opening. For example, during annealing the lateral cracks could grow at the expense of the radial crack system.

An important observation of the present work is that flaw healing cannot be characterized using optical techniques alone. In the case of the composite, the optical measurements indicated significant healing, while the SEM revealed only a small degree of true bonding. This disparity arises because the resolution limits of the optical technique are governed by the crack opening displacement. When the displacement at the crack tip is small, the optical technique cannot

resolve the correct position of the crack tip. A further limitation of the optical technique is evident from the alumina results. The crack growth that was evident using SEM was masked by the uncertainty in optical crack length measurements. Therefore, while it is relatively simple and productive to measure crack lengths optically, these measurements must be complemented with higher magnification images of the crack tips.

V. Conclusions

(1) The healing behavior of indentation cracks in Al_2O_3 and Al_2O_3-SiC nanocomposite are dissimilar. In the nanocomposite the cracks close during annealing, whereas in the alumina the cracks propagate slightly. An implication is that machining flaws also react differently on annealing, consistent with a previous hypothesis that explained the strengthening of nanocomposites by heat treatment.

(2) Indentation cracks do not necessarily heal during annealing. If a microstructural toughening mechanism is coupled to the temperature and relaxes more rapidly than the residual stress field decays, then the cracks may propagate.

(3) Grain-localized frictional tractions generated by thermal expansion anisotropy relax rapidly during heating of Al_2O_3, leading to growth of indentation cracks. The transgranular fracture path caused by the SiC particles in Al_2O_3-SiC suppresses the effect of these tractions and therefore the cracks heal.

(4) Optical crack-length measurements are not sufficient to characterize flaw healing behavior in ceramics. They must be complemented with high magnification observations of the crack tips.

Acknowledgements

We are grateful to L. C. Stearns and J. Zhao for providing the hot-pressed samples used in this study. This work was supported by the Office of Naval Research under grant # N00014-92-J-1635. P0002.

References

(1) K. Niihara and A. Nakahira, "Strengthening of Oxide Ceramics by SiC and Si_3N_4 Dispersions"; pp. 919-926 in *Proceedings of the Third International Symposium on Ceramic Materials & Components for Engines*. The American Ceramic Society, Westerville, OH 1988.

(2) K. Niihara, A. Nakahira, G. Sasaki, and M. Hirabayashi,"Development of Strong Al_2O_3 Composites"; pp. 124-134 in *Proceedings of the International Meeting on Advanced Materials*. Vol. 4. The Materials Research Society, Japan 1989.

(3) K. Niihara and A. Nakahira, "Particulate Strengthened Oxide Nanocomposites"; pp. 637-664 in *Advanced Structural Inorganic Composites*. Edited by P. Vincenzini. Elsevier Sci. Pub., Trieste, 1990.

(4) K. Niihara, "New Design Concept of Structural Ceramics - Ceramic Nanocomposites," The Centennial Issue of the Ceramic Society of Japan, *J. Ceram. Soc. Japan*, **99** [10] 974-982 (1991).

(5) L. C. Stearns, J. Zhao, and M. P. Harmer, "Processing and Microstructure Development in Al_2O_3-SiC "Nanocomposites"," *J. Eur. Ceram. Soc.*, **10** 473-477 (1992).

(6) J. Zhao, L. C. Stearns, M. P. Harmer, H. M. Chan, G. A. Miller and R. F. Cook, "Mechanical Behavior of Al_2O_3-SiC "Nanocomposites"," *J. Am. Ceram. Soc.*, **76** [2] 503-10 (1993).

(7) C.F. Yen and R. L. Coble, "Spheroidization of Tubular Voids in Al_2O_3 Crystals at High Temperatures," *J. Am. Ceram. Soc.*, **55** [10] 507-509 (1972).

(8) S. M. Park and D. R. O'Boyle, "Observations of Crack Healing in Sodium Chloride Single Crystals at Low Temperatures," *J. Mater. Sci. Lett.* **12** 840-841 (1977).

(9) A. H. Heuer and J. P. Roberts, "The Influence of Annealing on the Strength of Corundum Crystals," *Proc. Brit. Ceram. Soc.*, [6] 17-27 (1966).

(10) L. M. Davies, "The Effect of Heat Treatment on Tensile Strength of Sapphire," *ibid*, 29-53.

(11) H. P. Kirchner, R. M. Gruver and R. E. Walker, "Strength Effects Resulting from Simple Surface Treatments"; pp353-363 in *The Science of Ceramic Machining and Surface Finishing*. Edited by S. J. Schneider, Jr. and R. W. Rice. U.S. Government Printing Office, Washington DC 1972.

(12) B. J. Hockey and B.R. Lawn,"Electron Microscopy of Microcracking about Indentations in Aluminium Oxide and Silicon Carbide," *J. Mater. Sci.*, **10** 1275-84 (1975).

(13) D. H. Roach and A. R. Cooper, "Effect of Contact Residual Stress Relaxation on Fracture

Strength of Indented Soda-Lime Glass," *J. Am. Ceram. Soc.*, **68** [11] 632-636 (1985).

(14) J. Wang and R. Stevens, "Modification of Indentation Cracks in TZP ceramics by Thermal Treatment," *J. Mater. Sci. Lett.*, 7 560-562 (1988).

(15) P. Hrma, W.T. Han and A. R. Cooper, "Thermal Healing of Cracks in Glass," *J. Non-Cryst. Solids*, **102** 88-94 (1988).

(16) J. H. Cantrell, M. Qian, M. V. Ravichandran and K. M. Knowles, "Scanning Electron Acoustic Microscopy and Residual Stresses in Ceramics," *Appl. Phys. Lett.*, **57** [18] 1870-72 (1990).

(17) S. R. Choi and V. Tikare, "Crack Healing Behavior of Hot Pressed Silicon Nitride due to Oxidation," *Scripta metall. et mater.*, **26** 1263-1268 (1992).

(18) T. K. Gupta, "Crack Healing and Strengthening of Thermally Shocked Alumina," *J. Am. Ceram. Soc.*, **59** [5-6] 259-262 (1976).

(19) T. K. Gupta, "Instability of Cylindrical Voids in Alumina," *J. Am. Ceram. Soc.*, **61** [5-6] 191-195 (1978).

(20) T. K. Gupta, "Crack Healing in Al_2O_3, MgO and Related Materials"; pp. 750-766 in Advances in Ceramics Vol. 10, *Structure and Properties of MgO and Al_2O_3 Ceramics*. Edited by W. D. Kingery. American Ceramic Society, Columbus, OH, 1984.

(21) F. F. Lange and T. K. Gupta, "Crack Healing by Heat Treatment," *J. Am. Ceram. Soc.*, **53** [1] 54-55 (1970).

(22) F. F. Lange and K. C. Radford, "Healing of Surface Cracks in Polycrystalline Al_2O_3," *J. Am. Ceram. Soc.*, **53** [7] 420-421 (1970).

(23) G. Bandyopadhyay and J. T. A. Roberts, "Crack Healing and Strength Recovery in UO_2," *J. Am. Ceram. Soc.*, **59** [9-10] 415-419 (1976).

(24) G. Bandyopadhyay and C. R. Kennedy, "Isothermal Crack Healing and Strength Recovery in UO_2 Subjected to Varying Degrees of Thermal Shock," *J. Am. Ceram. Soc.*, **60** [1-2] 48-50 (1977).

(25) J. T. A. Roberts and B. J. Wrona, "Crack Healing in UO_2," *J. Am. Ceram. Soc.*, **56** [6] 297-299 (1973).

(26) Y. Ohya, Z. Nakagawa and K. Hamano, "Crack Healing and Bending Strength of Aluminum Titanate Ceramics at High Temperatures," *J. Am. Ceram. Soc.*, **71** [5] C-232-C-233 (1988).

(27) Y. Kim and E. D. Case, "Time-Dependent Elastic Modulus Recovery Measurement on Thermally Shocked SiC Fibre-Aluminosilicate Composites, Machinable Glass Ceramics and Polycrystalline Alumina," *J. Mater. Sci.*, **27** 1537-1545 (1992).

(28) J. Rödel and A. M. Glaeser, "Production of Controlled-Morphology Pore Arrays: Implications and Opportunities," *J. Am. Ceram. Soc.*, **70** [8] C-172-C-175 (1987).

(29) J. Rödel and A. M. Glaeser, "High-Temperature Healing of Lithographically Introduced Cracks in Sapphire," *J. Am. Ceram. Soc.*, **73** [3] 592-601 (1990).

(30) J. D. Powers and A. M. Glaeser, "High-Temperature Healing of Cracklike Flaws in Mg- and Ca- Ion-Implanted Sapphire," *J. Am. Ceram. Soc.*, **75** [9] 2547-58 (1992).

(31) J. D. Powers and A. M. Glaeser, "High-Temperature Healing of Cracklike Flaws in Titanium Ion-Implanted Sapphire," *J. Am Ceram. Soc.*, **76** [9] 2225-2234 (1993).

(32) A. G. Evans and E. A. Charles, "Strength Recovery by Diffusive Crack Healing," *Acta metall.*, **25** 919-927 (1977).

(33) E. D. Case, J. R. Smyth and O. Hunter Jr.,"Microcrack Healing During the Temperature Cycling of Single Phase Ceramics"; pp. 507-530 in *Fracture Mechanics of Ceramics*, Vol 5. Edited by R. C. Bradt, A. G. Evans, D. P. H. Hassleman and F. F. Lange. Plenum, New York, 1983.

(34) K. Jagannadham and J. Narayan, "Fracture Behavior of Laser-Modified Ceramic Materials," *Mater. Lett.*, **7** [9-10] 303-315 (1989).

(35) R. F. Cook, "Influence of Crack Velocity Thresholds on Stabilized Nonequilibrium Fracture," *J. Appl. Phys.*, **65** [5] 1902-1910 (1989).

(36) K.-T. Wan, N. Aimard, S. Lathabai, R. G. Horn and B. R. Lawn, "Interfacial Energy States of Moisture-Exposed Cracks in Mica," *J. Mater. Res.*, **5** [1] 172-182 (1990).

(37) K.-T. Wan, S. Lathabai and B. R. Lawn," Crack Velocity Functions and Thresholds in Brittle Solids," *J. Eur. Ceram. Soc.*, **6** 259-268 (1990).

(38) J. W. Obreimoff, "The Splitting Strength of Mica," *Proc. Roy. Soc. London*, **A127** 290-297 (1930).

(39) T. A. Michalske and E. R. Fuller, Jr., "Closure and Repropagation of Healed Cracks in Silicate Glass," *J. Am. Ceram. Soc.*, **68** [11] 586-590 (1985).

(40) Lord Rayleigh, "On the Instability of Jets," Proc. London Math Soc., **10** 4-13 (1878).

(41) F. A. Nichols and W. W. Mullins, "Morphological Changes of a Surface of Revolution due to Capillary-Induced Surface Diffusion," *J. Appl. Phys.*, **36** [6] 1826-1835 (1965).

(42) F. A. Nichols and W. W. Mullins, "Surface- (Interface-) and Volume-Diffusion Contributions to Morphological Changes Driven by Capillarity," *Trans. A. I. M. E.*, **233** 1840-1848 (1965).

(43) F. A. Nichols, "On the Speroidization of Rod-Shaped Particles on Finite Length," *J. Mater. Sci.*, **11** 1077-1082 (1976).

(44) F. A. Nichols, "Theory of Sintering of Wires by Surface Diffusion," *Acta metall.*, **16** 103-113 (1968).

(45) B. R. Lawn, A. G. Evans and D. B. Marshall, "Elastic/Plastic Indentation Damage in Ceramics: The Median/Radial Crack System," *J. Am. Ceram. Soc.*, **63** [9-10] 574-581 (1980).

(46) G. R. Anstis, P. Chantikul, B. R. Lawn, and D. B. Marshall, "A Critical Evaluation of Indentation Techniques for Measuring Fracture Toughness: I, Direct Crack Measurements," *J. Am. Ceram. Soc.*, **64** [9] 533-538 (1981).

(47) R. F. Cook and G. M. Pharr, "Direct Observation and Analysis of Indentation Cracking in Glasses and Ceramics," *J. Am. Ceram. Soc.*, **73** [4] 787-817 (1990).

(48) R. F. Cook and D. H. Roach, "The Effect of Lateral Crack Growth on the Strength of Contact Flaws in Brittle Materials," *J. Mater. Res.*, **1** [4] 589-600.

(49) J. E. Blendell and R. L. Coble, "Measurement of Stress Due to Thermal Expansion Anisotropy in Al_2O_3," *J. Am. Ceram. Soc.*, **65** [3] 174-178 (1982).

(50) A. G. Evans and Y. Fu, "Microstructural Residual Stresses," pp 137-153 in *Fracture in Ceramic Materials*; Edited by A. G. Evans, Noyes, New Jersey (1984).

(51) S. J. Bennison and B. R. Lawn, "Role of Interfacial Grain-Bridging Sliding Friction in the Crack-Resistance and Strength Properties of Nontransforming Ceramics," *Acta metall.*, **37** [10] 2659-2671 (1989).

(52) D. Johnson-Walls, M. D. Drory, A. G. Evans, D. B. Marshall, and K. T. Faber, "Evaluation of Reliability of Brittle Components by Thermal Stress Testing," *J. Am. Ceram. Soc.*, **68** [7] 363-67 (1985).

(53) R. F. Cook, M. R. Pascucci, and W. H. Rhodes, " Lateral Cracks and Microstructural Effects in the Indentation Fracture of Yttria," *J. Am. Ceram. Soc.*, **73** [7] 1873-78 (1990).

(54) M. V. Swain, "R-curve behaviour in a polycrystalline alumina material," J. Mater Sci. Lett., 5 1313-1315 (1986).

(55) R. Knehans and R. Steinbrech, "Memory Effect of Crack Resistance During Slow Crack Growth in Notched Al_2O_3 Bend Specimens," *J. Mater. Sci. Lett.*, 1 327-329 (1982).

(56) C. J. Fairbanks, B. R. Lawn, R. F. Cook and Y-W. Mai, " Microstructure and Strength of Ceramics"; pp. 23-37 in *Fracture Mechanics of Ceramics* Vol 8. Edited by R. C. Bradt, A. G. Evans, D. P. H. Hassleman and F. F. Lange. Plenum, New York 1986.

(57) P. L. Swanson, C. Fairbanks, Y-W Mai, B. R. Lawn and B. J. Hockey, "Crack-Interface Grain Bridging as a Fracture Resistance Mechanism in Ceramics: I, Experimental Study on Alumina," *J. Am. Ceram. Soc.*, **78** [4] 279-89 (1987).

(58) S. M. Wiederhorn, B. J. Hockey and D. E. Roberts, "Effect of Temperature on the Fracture of Sapphire," *Phil. Mag.*, **28** [4] 783-796 (1973).

(59) M. Iwasa and R. C. Bradt, "Fracture Toughness of Single-Crystal Alumina"; pp. 767-779 in Advances in Ceramics Vol. 10, *Structure and Properties of MgO and Al_2O_3 Ceramics*. Edited by W. D. Kingery. American Ceramic Society, Columbus, OH, 1984.

(60) A. G. Evans, M. Linzer and L. R. Russell, "Acoustic Emission and Crack Propagation in Polycrystalline Alumina, " *Mat. Sci. and Eng.*, **15** 253-261 (1974).

Table I: Indentation crack lengths for Al_2O_3 and Al_2O_3-SiC.

Al_2O_3

Indentation Load (N)	c (μm) (As indented)	c (μm) (Immediately prior to annealing)	c (μm) (Immediately after annealing)
10	58 ± 7	58 ± 6	62 ± 7
50	195 ± 26	191 ± 18	200 ± 40
100	291 ± 48	300 ± 40	315 ± 41

Al_2O_3-SiC

Indentation Load (N)	c (μm) (As indented)	c (μm) (Immediately prior to annealing)	c (μm) (Immediately after annealing)
10	52 ± 3	51 ± 4	39 ± 5
50	147 ± 13	147 ± 11	118 ± 12
100	239 ±13	239 ± 13	203 ± 15

Figure Captions

Figure 1. Plot of inert strength as a function of indentation load for hot-pressed, annealed Al_2O_3-SiC composite (HC-A) and hot-pressed unannealed composite (HC-U). The schematic drawings show the proposed effect of annealing the specimen surface: The residual stress layer is relaxed and the flaw size is reduced. After Zhao et al.[6]

Figure 2. Schematic diagram of the experimental procedure used for characterizing the crack-healing behavior.

Figure 3. Optical micrographs of 50 N indentations in (A) as-indented and (B) annealed Al_2O_3-SiC nanocomposite, and (C) as-indented and (D) annealed Al_2O_3. The arrows indicate the crack tips.

Figure 4. Crack length, c_o, and indentation semi-diagonal, a, as a function of indentation load, P, for (A) Al_2O_3-SiC nanocomposite and (B) Al_2O_3. The solid lines are best fits to the data, consistent with constant toughness and hardness. The dashed line is an empirical fit.

Figure 5. SEM images of an uncoated Al_2O_3-SiC nanocomposite (A) prior to, and (B) after annealing for 2 h at 1300 °C in argon. The crack emanated from one corner of a 10 N Vickers indentation. The crack opening displacements measured from these images are given in (C).

Figure 6. SEM images of an uncoated Al_2O_3 (A) prior to, and (B) after annealing for 2 h at 1300 °C in argon. The crack emanated from one corner of a 50 N Vickers indentation. The crack opening displacements measured from these images are given in (C).

Figure 7. Schematic diagram depicting the crack tip in Al_2O_3-SiC (A) after indenting (and during heating to the annealing temperature) and (B) after annealing. K_r represents the residual stress-intensity factor wedging open the crack.

Figure 8. Schematic diagram depicting the crack tip in Al_2O_3 (A) after indenting, (B) during heating to the annealing temperature, and (C) after annealing. K_r represents the residual stress intensity factor wedging open the crack, and σ_f represents the frictional tractions arising from the thermal expansion anisotropy.

Fig 1

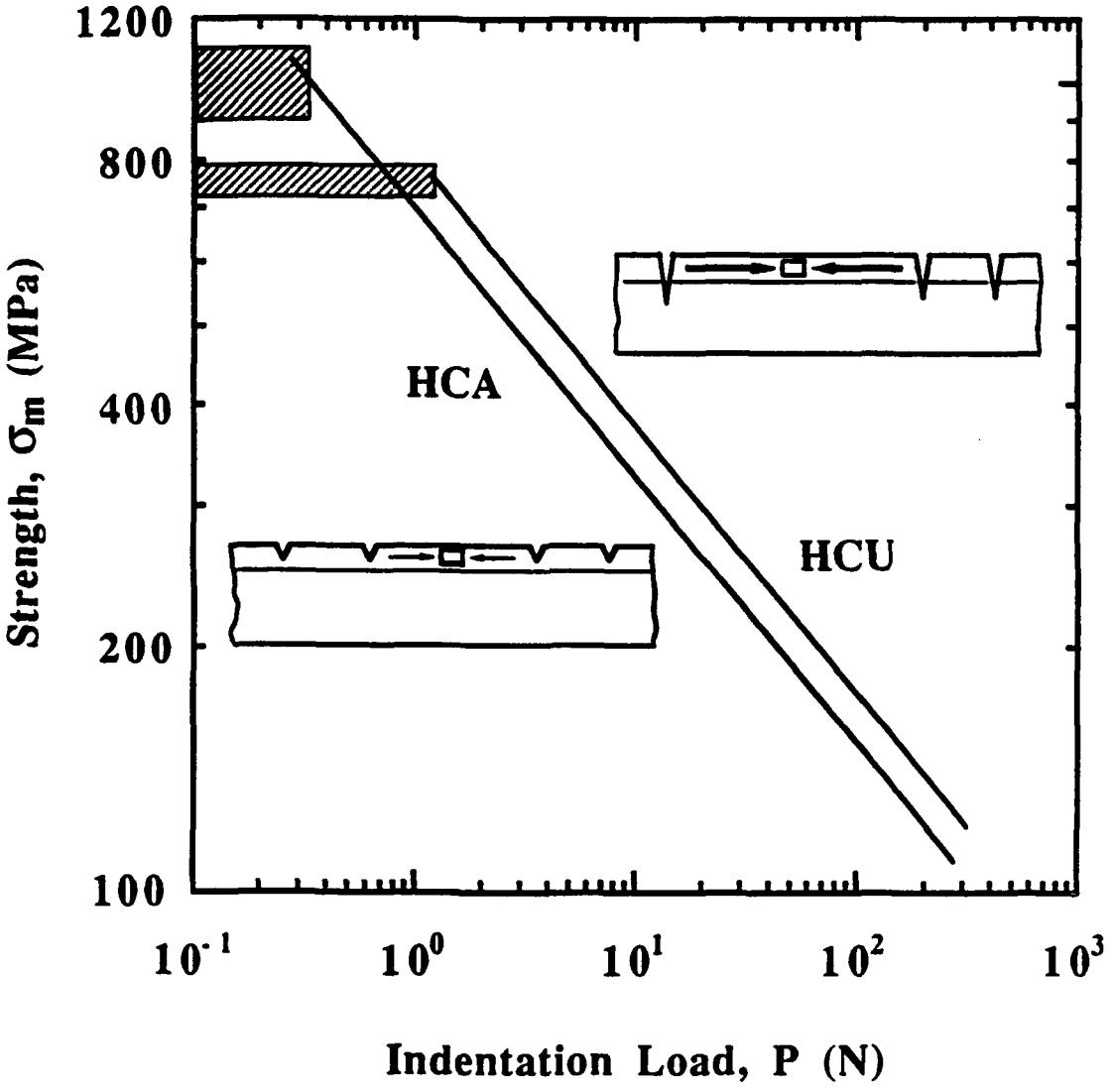
1200
800
400
200
100
Strength, σ_m (MPa)
HCA
HCU
10^{-1}
10^0
10^1
10^2
10^3
Indentation Load, P (N)

Fig 2.

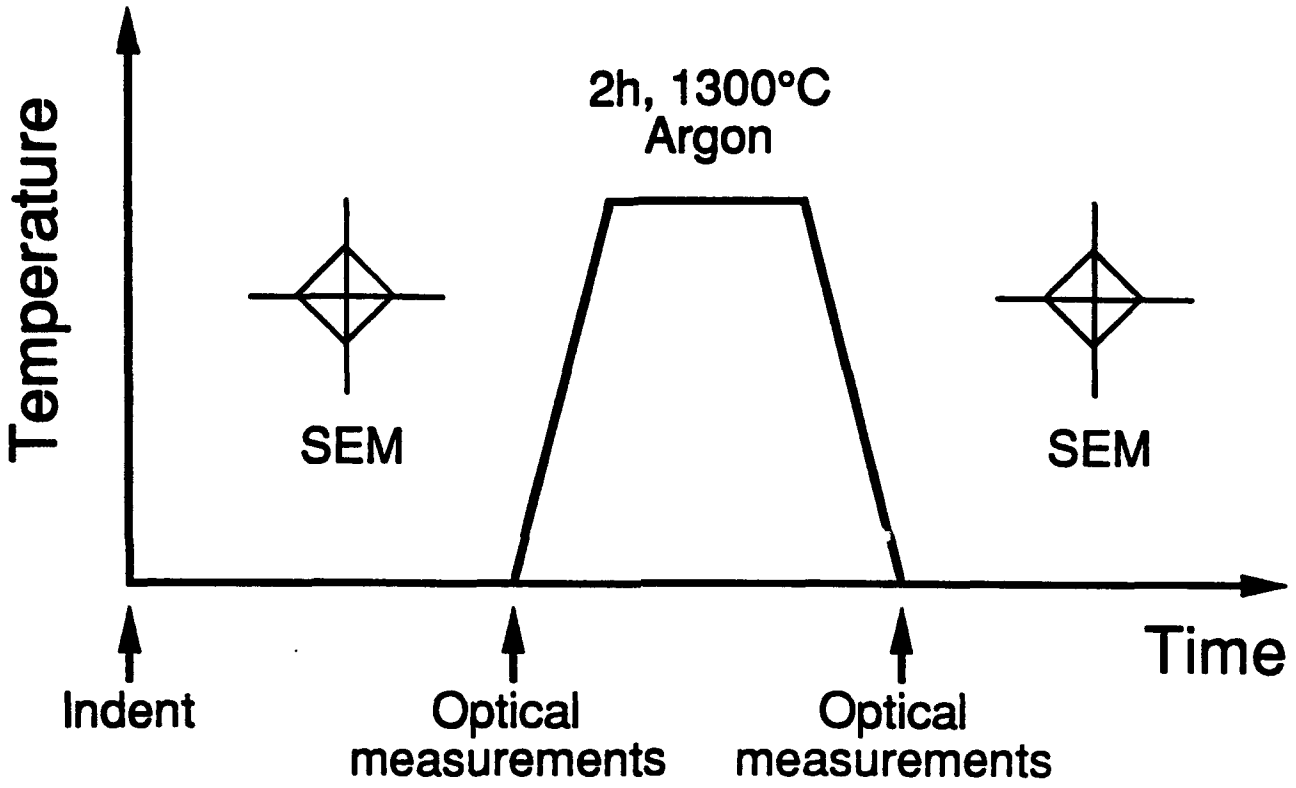
Temperature
2h, 1300°C
Argon
SEM
SEM
Time
Indent
Optical
measurements
Optical
measurements

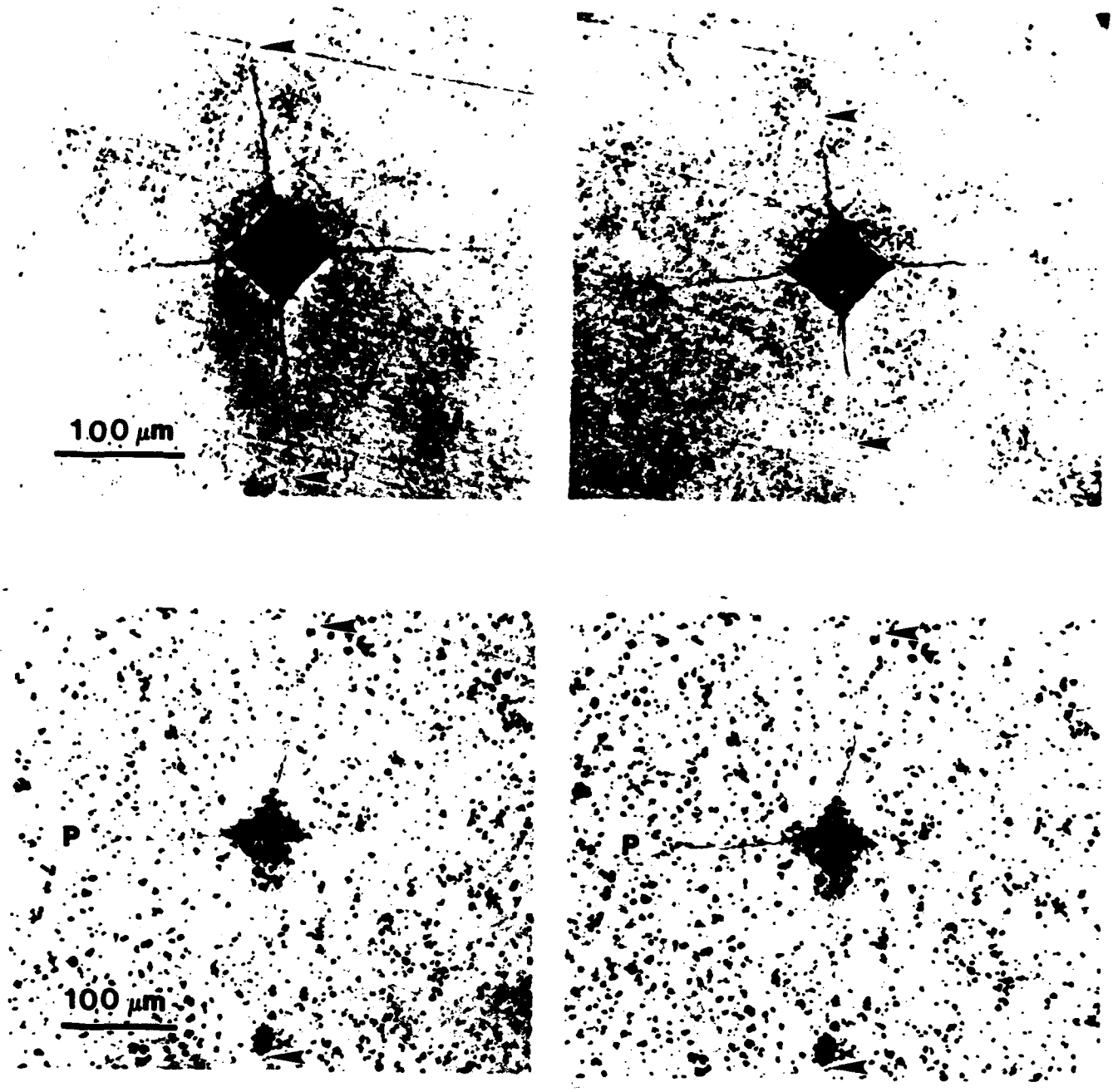

Figure 3.

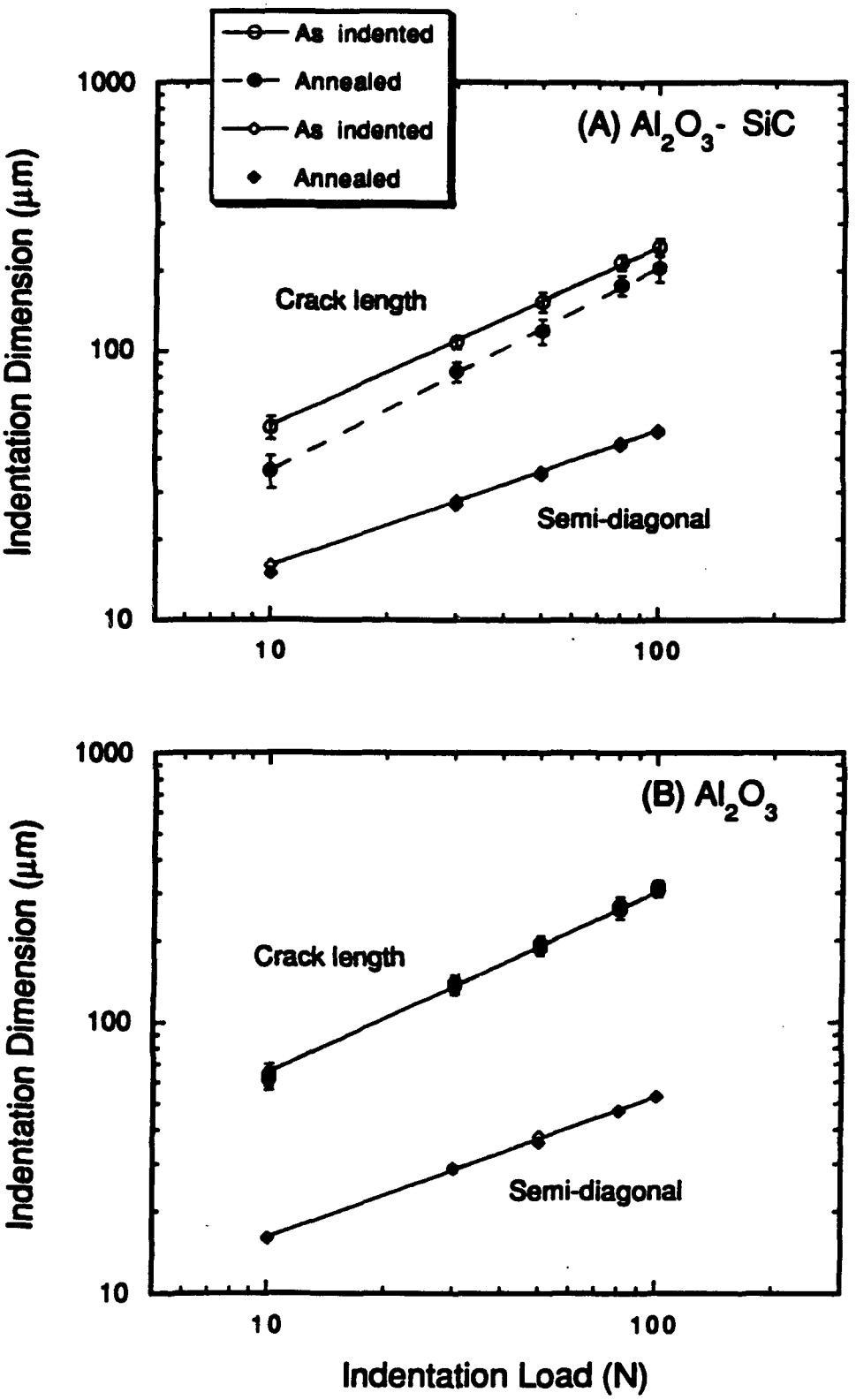
As indented
Annealed
As indented
Annealed
(A) Al_2O_3- SiC
Crack length
Semi-diagonal
Indentation Dimension (μm)
1000
100
10
10
100
(B) Al_2O_3
Crack length
Semi-diagonal
Indentation Dimension (μm)
1000
100
10
10
100
Indentation Load (N)

Fig 4.

Figure 5.

(A)
(B)
(C)
1μm
1μm
Crack Opening Displacement (μm)
0.12
0.1
0.08
0.06
0.04
0.02
0
0
2
4
6
8
10
Distance along Crack (μm)

Figure 6

(A)
(B)
(C)
3 μm
3 μm
Crack Opening Displacement (μm)
0
0.1
0.2
0.3
0.4
0.5
0.6
0.7
0
4
8
12
16
20
24
28
Distance along Crack (μm)

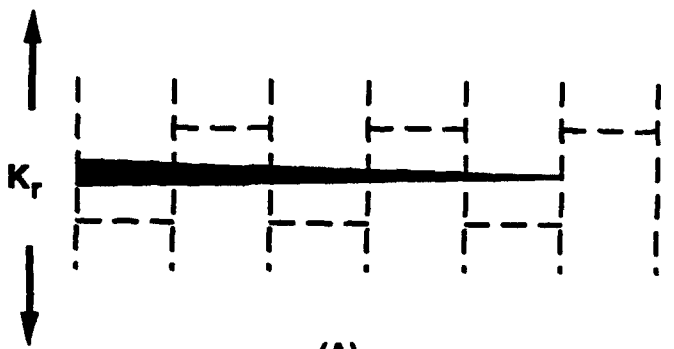

(A)

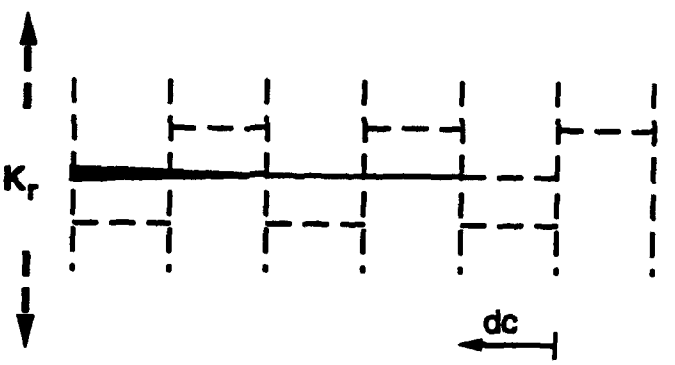

(B)

Fig 7.

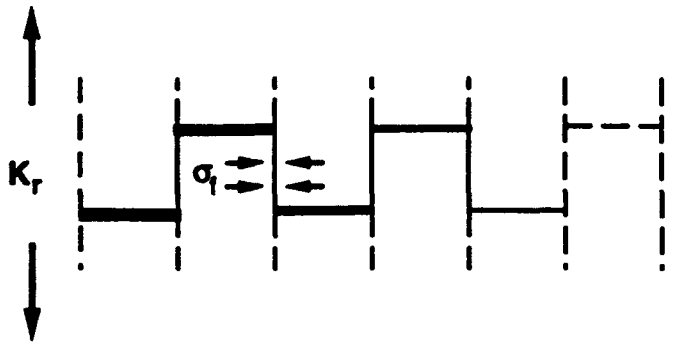

(A)

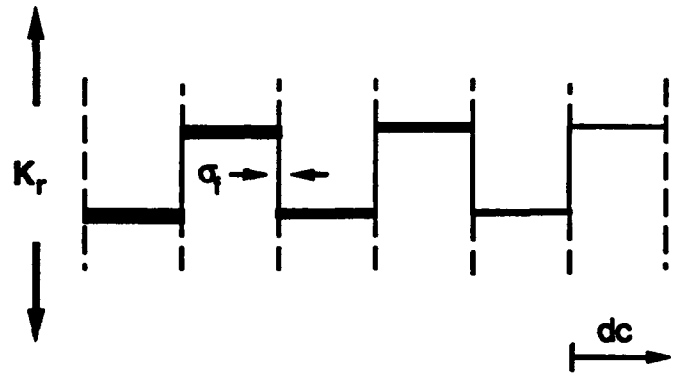

(B)

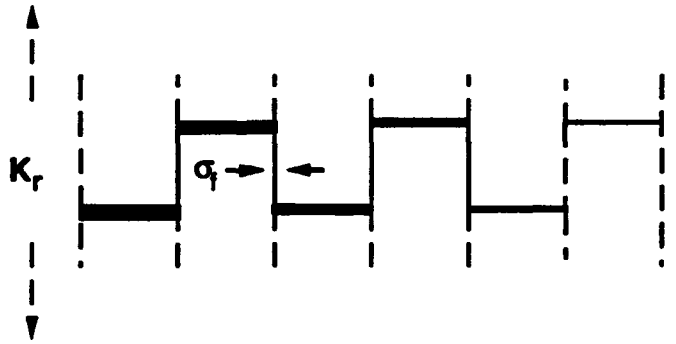

(C)

Fig 8.

Section 1.2

APPLICATION OF SCANNING ELECTRON MICROSCOPY TO THE STUDY OF MULTI-PHASED CERAMIC COMPOSITES

by

Helen M. Chan, Martin P. Harmer, and Gary A. Miller

Proc. 51st Annual Meeting of the Micrscopy Society of America,
San Francisco Press, San Francisco, CA, 1993.

G. W. Bailey and C. L. Rieder, Eds., Proc. 51st Annual Meeting of the Microscopy Society of America

TITLE ➡

APPLICATION OF SCANNING ELECTRON MICROSCOPY TO THE STUDY OF MULTI-PHASE CERAMIC COMPOSITES

Helen M. Chan, Martin P. Harmer and Gary A. Miller

Materials Research Center and Dept. of Materials Science & Engineering, Lehigh University, Bethlehem, PA 18015

Recent on-going research at Lehigh has focussed on the tailoring of multi-phase ceramic composite structures for enhanced mechanical behavior. Results have shown that by suitable control of the morphology and nature of the phases present, improvements may be obtained in properties such as microstructural stability, flaw tolerance, and strength[1]. What follows is a brief discussion of examples illustrating applications of scanning electron microscopy (SEM) to this type of study for several specific systems.

Work by French et al.[2] revealed that relative to single phase materials, duplex structures (which consist of ~ 50:50 vol.% mixtures of mutually insoluble phases) show significantly enhanced resistance to grain coarsening. It was postulated that the slower grain growth rate in the duplex material resulted from the necessity for long-range diffusion. To test this hypothesis, the grain growth behavior of two duplex Al_2O_3:ZrO2 materials was compared, the difference being that a grain boundary glassy phase was deliberately incorporated into one of the structures. As can be seen from Figure 1, the intergranular glass behaved as a rapid pathway for diffusion, hence resulting in greater grain growth compared to the glass-free composite.

Figure 2 shows a SEM micrograph of an alumina composite containing 25 vol.% of calcium hexaluminate ($CaAl_{12}O_{19}$). As clearly illustrated by Figure 2B, the hexaluminate phase forms dispersed plate-like grains. Preliminary measurements using the indentation-strength-in-bending technique reveal that the composite shows superior strength behavior over a wide range of flaw sizes. Examination of indentation cracks in the material indicates that this results from the hexaluminate grains behaving as crack bridging sites.

The work of Niihara et al.[3], which showed that alumina composites containing fine dispersions of SiC particles can exhibit significantly improved fracture strengths (> 1500 MPa), has excited much interest in these materials[4]. Figure 3 shows the morphology of the same indentation crack in an Al_2O_3:5 vol.% SiC composite, both before and after annealing. Careful comparison of Figs. 3A and 3B reveals evidence of crack closure, and possibly crack healing. Interestingly, this is not observed for cracks in single phase alumina. Research is currently underway to rationalize this difference in behavior, and relate it to bulk mechanical properties.

References

1. M.P. Harmer, H.M. Chan and G.A. Miller, J. Am. Ceram. Soc. (1992)75, 1715
2. J.D. French et al., J. Am. Ceram. Soc. (1990)73, 2508
3. K. Niihara and A. Nakahira, in "Advanced Structural Inorganic Composites", Ed. P. Vincenzi, Elsevier, 1990, pp. 637-64
4. J. Zhao et al., J. Am. Ceram. Soc. (1993)76 [illegible]

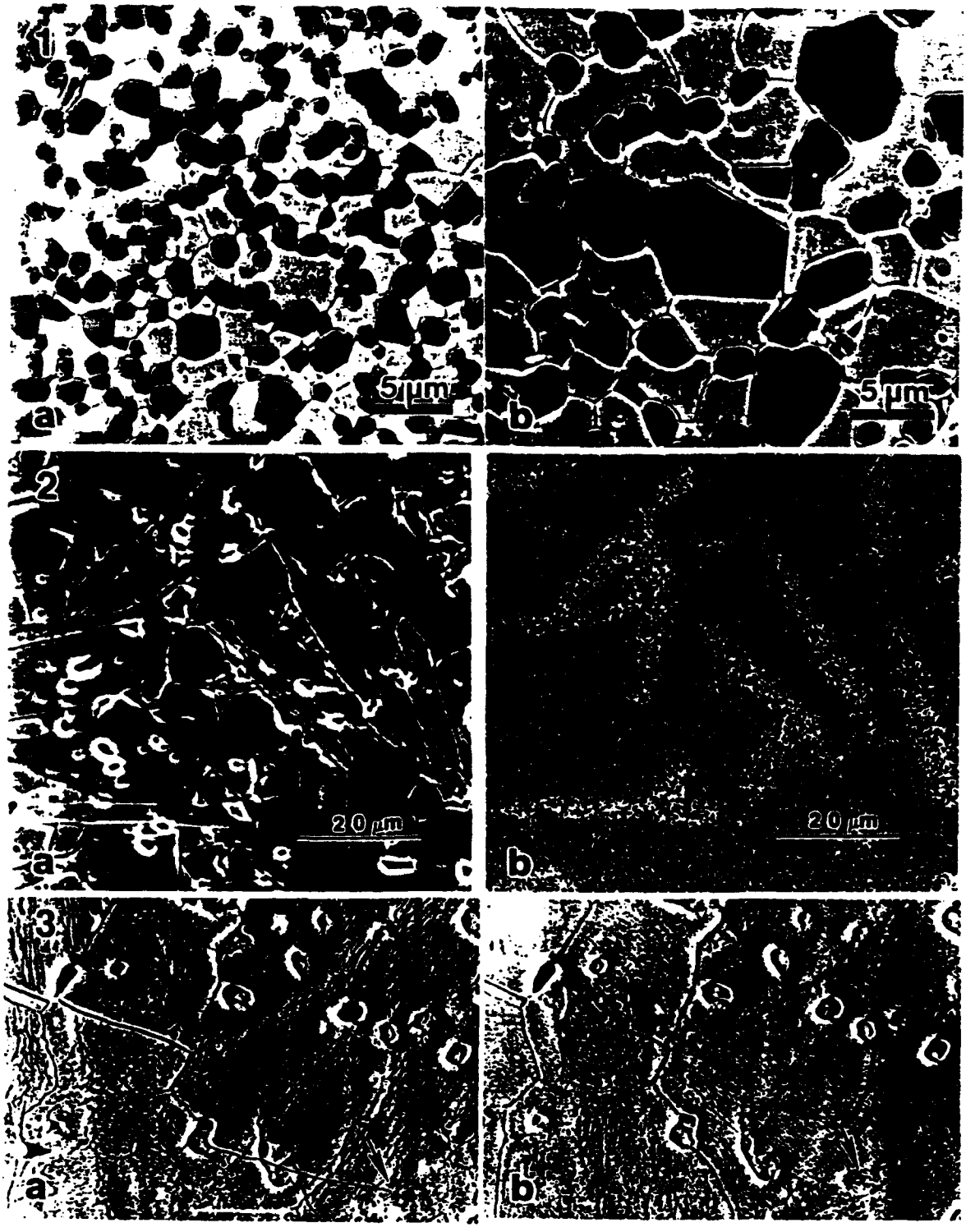

FIG. 1.--SEM micrograph showing microstructure after annealing 65 h at 1600 °C . A) Al_2O_3:50 vol.% c-ZrO_2, B) Al_2O_3:50 vol.% c-ZrO_2 + 1 vol. % anorthite glass (and 0.1 wt.% MgO). Courtesy S. Dill and J.D. French.

FIG. 2.--A) SEM micrograph of Al_2O_3:25 vol.% $CaAl_{12}O_{19}$ (+ 1 vol.% anorthite glass), B) Calcium K-α x-ray map of same region. Courtesy L. An.

FIG. 3.--SEM micrograph of the tip region of an indentation crack in an Al_2O_3:5 vol.% SiC composite. (Uncoated, operating voltage 3.1 keV). A) As indented, B) After annealing for 2 h at 1300 °C in an Argon atmosphere. Courtesy M. Thompson.

Section 1.3

RESIDUAL STRESS RELAXATION BEHAVIOR IN Al_2O_3-SiC NANOCOMPOSITES

by

J. Fang, A. M. Thompson, I. A. Chou, H. M. Chan, and M. P. Harmer

TECHNICAL PROGRESS REPORT

Residual Stress Relaxation Behavior in Al_2O_3-SiC Nanocomposite

J. Fang, A. M. Thompson, I. A. Chou, H. M. Chan and M. P. Harmer

I. Introduction

In recent years, there has been a growing interest in a class of nanocomposite materials typified by the Al_2O_3-SiC system. Niihara *et al.* [1-4] first discovered that the addition of 5 vol.% sub-micron SiC particles to Al_2O_3 not only increased the strength from 380 MPa to 1000 MPa, but also improved the toughness by 40%. Furthermore, it was shown that a simple annealing procedure increased the strength to over 1500 MPa. However, the mechanism(s) responsible for the beneficial effects of SiC particles and the subsequent annealing treatment are not well understood.

Subsequent work by Zhao *et al.* [5] has shown that the nanocomposite exhibited superior mechanical properties compared to Al_2O_3 only if the samples had been subjected to industrial grinding. After annealing for 2 hours at 1300^0C, the strength of the nanocomposite was increased to about 1000 MPa. While there was a slight increase in the toughness, the increase was not sufficient to account for the increase in the strength. Consequently, these workers have attributed the enhancement of mechanical properties in the nanocomposite to the compressive residual surface stresses introduced by the grinding process. It was further hypothesized that, during annealing of the nanocomposite, the intrinsic (unindented) strength was increased mainly due to the healing of machining induced cracks, and that the slight apparent increase in toughness was due to retained residual stresses. Recently, the indentation study by Thompson *et al.* [6] corroborated the crack healing hypothesis.

The present work was directed at testing the residual stress hypothesis. Residual stress relaxation in Al_2O_3 and Al_2O_3/SiC nanocomposite has been studied using two approaches. First, an indentation technique was employed whereby the stress field around

a large Vickers indentation is mapped by the cracking behavior at smaller "satellite" indents. Second, preliminary TEM observations were made to characterize and compare the deformation structures in alumina and the nanocomposite, and to determine how such structures are influenced by annealing.

II. Experimental

Indentation experiments were performed on both hot-pressed and pressureless sintered single phase Al_2O_3, and Al_2O_3 containing 5 vol.% 0.15 μm SiC particles. These materials are identical to those utilized in the study by Zhao *et al.* [5] and details of the processing techniques have been described elsewhere [7]. Since the processing method did not change the crack behavior, no distinction will be made between the hot-pressed and the pressureless sintered materials.

Sample surfaces were prepared by grinding and polishing down to 1 μm diamond grit size. Indentations were made on the polished surface using a Vickers diamond pyramid. Two different conditions were used for each material. One condition was that a large indent was placed in a sample and four small indents were then put nearby the first indent. The other condition was that a larger indent was put in a sample but the sample was annealed before introducing the four satellite indents. For simplicity, the former condition will be termed "as-indented" and the latter "annealed". The indentation load was 100 N for the large indent and 5 N for the small indents. The descent and dwell time of the indentor was 15 s. The annealing was carried out at 1300^0C in flowing argon for 2 hours, which was the same procedure used by Niihara *et al.* [3] and Zhao *et al.* [5].

TEM observations were made only on hot-pressed materials. Disks of 3 mm in diameter were cut using an ultrasonic drill from bulk samples. The disks were ground and polished to a thickness of about 100 μm. The final polishing step was carried out using 1 μm diamond paste to remove any remnant grinding damage. Microhardness indentations were made using a Vickers diamond indenter with a load of 100 g. The disks were then

ion-beam thinned from one side only in order to retain the original indented or polished surface. Following carbon coating, the thin foils were examined in the TEM at 120 kV.

III. Results and discussion

3.1 Indentation observations

Fig. 1 shows the interaction between the large indent and the small indents in the "as indented" Al_2O_3 (Fig. 1a) and the nanocomposite (Fig. 1b). Clearly, the radial crack configurations of the small indentations are not symmetrical. For each small indent, only one pair of cracks were observed. Thus, the pair of cracks oriented in the radial direction of the large impression were distinct, whereas the pair oriented tangentially to the large impression were absent. The asymmetry in the radial crack behavior of the small indents is caused by residual stresses around the central indentation. The circumferential tensile residual stress due to the large indentation assists the propagation of the radially oriented cracks, whereas the radial compressive stress from the large indent suppresses the tangentially oriented cracks. In addition, the lengths of the cracks from the satellite indents were similar for both Al_2O_3 and the composite, which indicate that the residual stresses around the large indent were similar for both Al_2O_3 and the composite in the "as indented" condition.

Different crack behavior was observed for Al_2O_3 (Fig. 2a) and the composite (Fig. 2b) under the "annealed" condition. For Al_2O_3, the four radial cracks emanating from the corners of the small impressions were symmetrical in length, while for the composite, the radial crack lengths were still asymmetrical. It should be noted that the cracks at the small indents in the "annealed" condition were shorter than those in the "as indented" condition. These observations provide convincing evidence that, upon annealing, the residual stresses in Al_2O_3 were *completely* relaxed, whereas these stresses were only *partially* relieved in the composite.

Previous investigations [8-10] have showed that significant compressive residual surface stresses can be introduced by grinding processes, and that such stresses can cause apparent toughening in ceramics [11-13]. Since the grinding process may be regarded as the cumulative manifestation of a vast number of related "indentation events", given the results of the present study, it is reasonable to expect that the grinding-induced stress relief would be more difficult in the nanocomposite material, hence supporting the previous hypothesis proposed by Zhao *et al.* [5].

3.2 TEM observations

An important question that arises from the above indentation observations is by what mechanism(s) do the SiC particles inhibit the stress relaxation? To answer this question, TEM was used to examine the original industrially ground and annealed samples studied by Zhao et al.

The results showed that the two materials exhibited different structures. Specifically, in Al_2O_3, dislocation-free subgrains (Fig. 3a and b) were formed in most areas, while in the nanocomposite, a high density of tangled dislocations was observed (Fig. 4). This difference in the microstructure can be understood in terms of the pinning effect of SiC particles. In Al_2O_3, dislocations are able to move away from the heavily deformed areas and rearrange to form networks. During prolonged annealing, these networks would develop into subgrains. In contrast, in the nanocomposite, SiC particles would inhibit dislocation motion and prevent network formation. These observations are consistent with x-ray residual stress measurement on the polished surfaces [14].

In addition, TEM has been used to examine the dislocation structures generated by Vickers indentation in order to study the effects of contact deformation and subsequent annealing in a more controlled manner.

Fig. 4a shows the immediate vicinity of an indentation impression in the composite. Plastic deformation occurred by both slip and twinning. The density of dislocations

associated with the indentation was so high that individual dislocations could not be resolved. Microcracks (arrowed) were observed to form at some of the interfaces between the SiC particles and the Al_2O_3 matrix. After annealing at 1300°C, the dislocation density in the nanocomposite was still quite high. The micrograph (Fig. 4b) taken away from the impression clearly shows the inhibition of dislocation motion by SiC particles. It is believed that SiC particles inhibit dislocation rearrangement and, therefore, limit residual stress relaxation in the nanocomposite. Corresponding work on indentations in single phase alumina is in progress.

IV. Conclusions

1. The residual stress field introduced by a Vickers indentation was similar for both Al_2O_3 and the nanocomposite. Annealing for 2 hours at 1300°C completely relaxed the residual stresses surrounding the indentation in Al_2O_3, but only partially relieved the stresses in the nanocomposite.

2. TEM examination of industrially ground/annealed samples revealed that during annealing, dislocation-free subgrains were formed in Al_2O_3, whereas a high density of tangled dislocations were observed in the nanocomposite.

3. Preliminary TEM observations of indentations showed that plastic deformation occurred by both slip and twinning. During annealing, SiC particles inhibited dislocation motion. It is believed that this retardation of recovery processes accounts for the retention of the residual stresses induced during machining.

V. References

1. K. Niihara and A. Nakahira, "Strengthening of Oxide Ceramics by SiC and Si_3N_4 Dispersions", pp. 919-926 in Proceedings of the Third International Symposium on Ceramic Materials & Components for Engines, The American Ceramic Society, Westerville, OH (1988).

2. K. Niihara, A. Nakahira, G. Sasaki and M. Hirabayashi, "Development of Strong Al_2O_3/SiC Composites", pp. 124-134 in Proceedings of the International Meeting on Advanced Materials, vol. 4, The Materials Research Society, Japan (1989).

3. K. Niihara and A. Nakahira, "Particulate Strengthened Oxide Nanocomposites", pp. 637-664 in Advanced Structural Inorganic Composites, Edited by P. Vincenzini, Elsevier Sci, Pub. (1990).

4. K. Niihara, "New Design Concept of Structural Ceramics-Ceramic Nanocomposites,", the Centennial Issue of the Ceramic Society of Japan, 99 [10] 974-982 (1991).

5. J. Zhao, L. C. Stearns, M. P. Harmer, H. M. Chan, G. A. Miller and R. F. Cook, "Mechanical Behavior of Al_2O_3-SiC 'Nanocomposites' ", J. Am. Ceram. Soc. **76**, 503-510 (1993).

6. A. M. Thompson, H. M. Chan, M. P. Harmer and R. F. Cook, "Crack Healing and Stress Relaxation in Al_2O_3-SiC 'Nanocomposites' ", submitted to J. Am. Ceram. Soc.

7. L. C. Stearns, J. Zhao and M. P. Harmer, "Processing and Microstructure Development in Al_2O_3-SiC 'Nanocomposites' ", J. Eur. Ceram. Soc. 10, 473-477 (1992).

8. J. Lankford and D. L. Davidson, "Characterization of Surface Damage in Ceramics Using Selected Area Electron Channeling", pp. 395-405 in The Science of Ceramic Machining and Surface Finishing II, Edited by B. J. Hockey and R. W. Rice, US Government Printing Office, Washington, D.C. (1979).

9. F. F. Lange. M. R. James, and D. J. Green, "Determination of Residual Surface Stresses Caused by Grinding in Polycrystalline Al_2O_3", J. Am. Ceram. Soc. [2], C16-C17 (1983).

10. D. Johnson-Walls, A. G. Evans, D. B. Marshall and M. R. James, "Residual Stresses in Machined Ceramic Surfaces", J. Am. Ceram. Soc. 69 [1], pp. 44-47 (1986).

11. R. F. Cook, B. R. Lawn, T. P. Dabbs, and P. Chantikul, "Effect of Machining Damage on the Strength of a Glass-Ceramic", J. Am. Ceram. Soc. 64 [2], C121-C122 (1981).

12. D. B. Marshall, A. G. Evans, B. T. K. Yakub, J. W. Tien and G. S. Kino, "The Nature of Machining Damage in Brittle Materials", Proc. R. Soc. Lond. A385, pp. 461-475 (1983).

13. Y. Matsuo, T. Ogasawara, S Kimura, S. Sato and E. Yasuda, "The Effects of Annealing on Surface Machining Damage of Alumina Ceramics", J. Ceram. Soc. Japan 99, pp. 371-376 (1991).

14. J. Fang, A. M. Thompson, I. Chou, M. P. Harmer and H. M. Chan, "Microstructures of Al_2O_3-SiC Nanocomposite", 1992 ONR Annual Report.

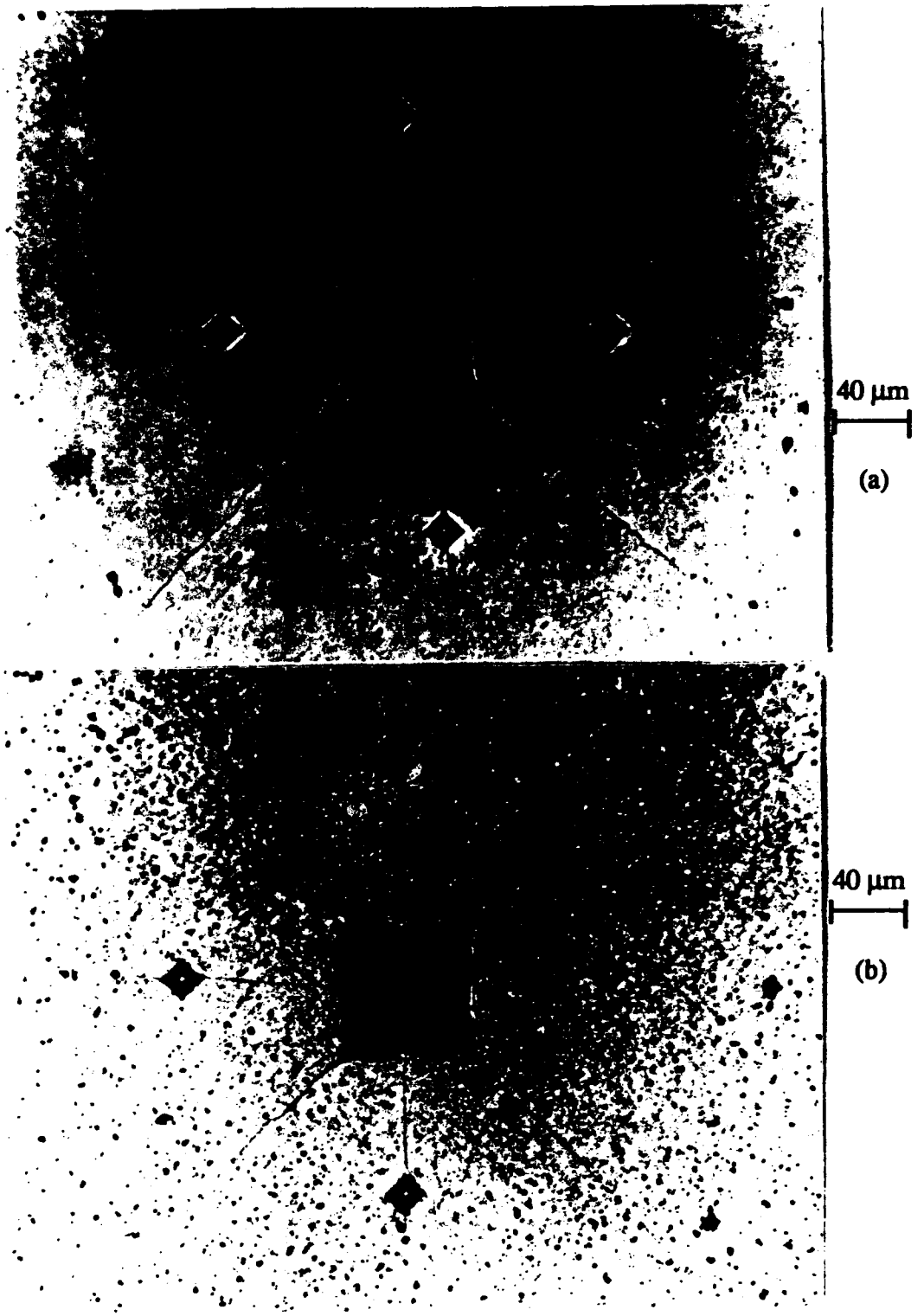

Fig. 1. Interaction between the small indents and the large intent in the "as indented" (a) Al_2O_3 and (b) the nanocomposite. The asymmetry in the radial crack configuration of the small indentations is a consequence of the residual stress field introduced by the indentation. The similarity in the length of these cracks indicates that the magnitude of the stresses for both materials was comparable.

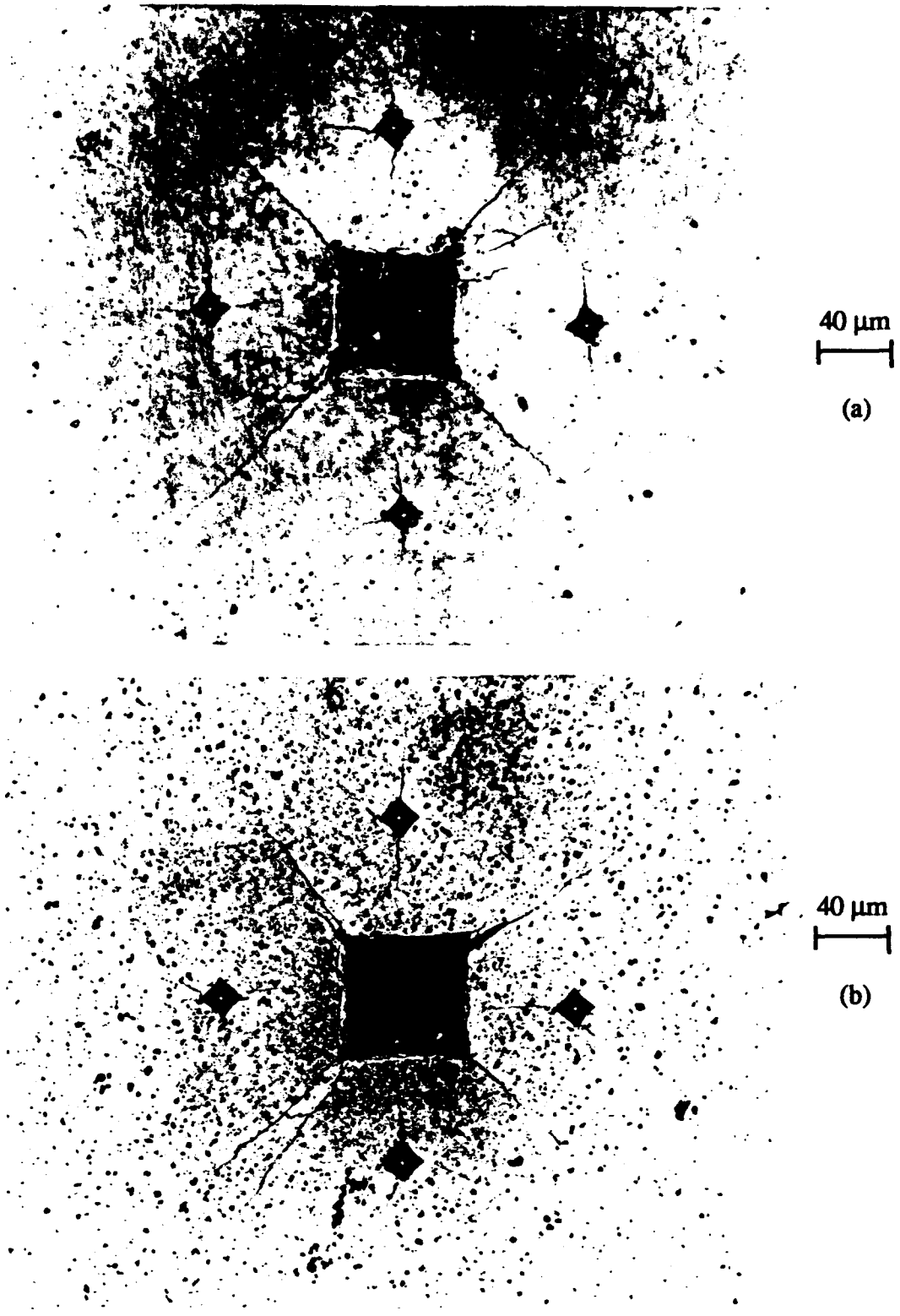

Fig. 2 showing that, under the "annealed condition", the radial crack configurations of the small impressions are symmetrical in Al_2O_3 (a), whereas those in the nanocomposite are asymmetrical (b), indicating that while the residual stresses are completely relaxed in Al_2O_3, these stresses were only partially relieved in the nanocomposite.

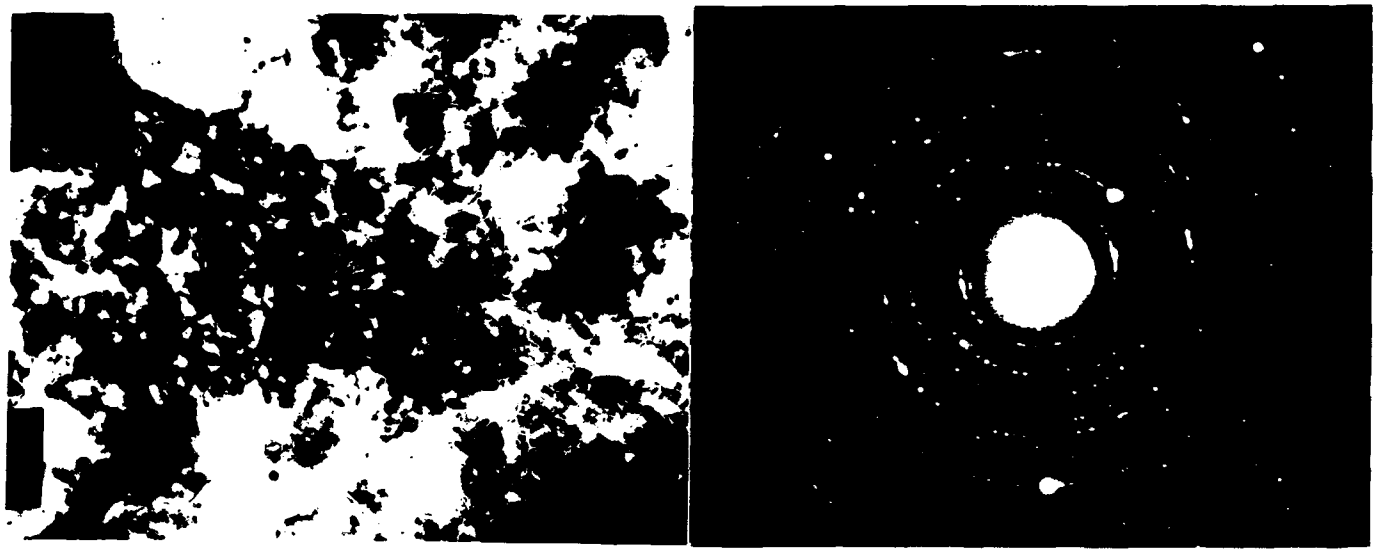

Fig. 3. TEM micrograph of the industrially ground/annealed surfaces in Al_2O_3 (a). Fig. (b) showing the diffraction pattern from the area in (a).

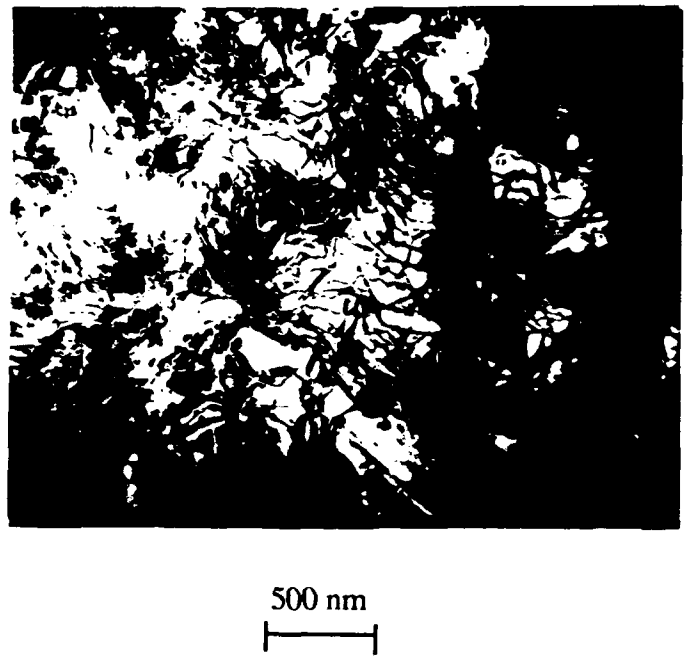

Fig. 4. TEM images of the industrially ground/annealed surface in the composites.

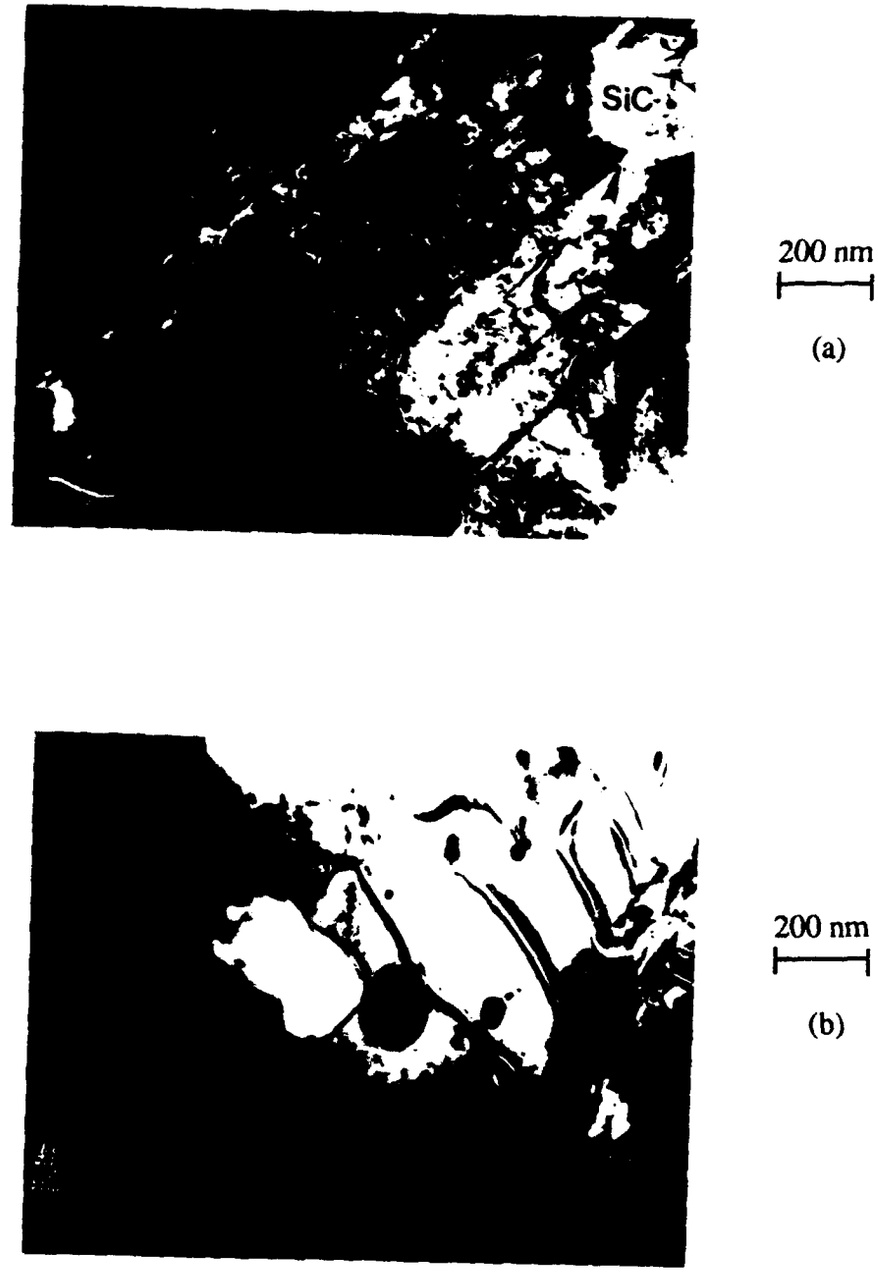

Fig. 5. TEM images of (a) indented and (b) indented/annealed in the nanocomposite.

Section 1.4

EFFECT OF SURFACE RESIDUAL STRESS ON NANOCOMPOSITES

by

I. A. Chou, J. Fang, A. M. Thompson, H. M. Chan, and M. P. Harmer

TECHNICAL PROGRESS REPORT

Effect of Surface Residual Stress on Nanocomposites

I. A. Chou, J. Fang, A. M. Thompson, H. M. Chan, and M. P Harmer

I. Introduction

In the recent years, studies by Niihara and his coworkers [1-4] have shown that an addition of 5 vol.% sub-micron SiC particles can significantly improve both the strength and toughness of Al_2O_3. In addition, the strength of the composite is further increased by a simple annealing treatment at 1300 °C for 2 hours. Similar studies by Zhao et al. [5,6] at Lehigh have suggested that such a strength increment is derived from surface residual stresses introduced by industrial grinding rather than an actual increase of the intrinsic material toughness. Consequently, the purposes of this current research are (1) to examine the influence of machining induced residual stress on the strength of Al_2O_3 - SiC composites, and (2) to study the effect of annealing on the subsequent relaxation of such stress.

II. Preparation of Materials

Five vol% of SiC were added to the Al_2O_3 starting powder, and the mixture ultrasonically dispersed and ball milled in methanol. The slurry was then slowly dried in air to produce uniform powder. Disk specimens were prepared by uniaxial cold pressing at 75 MPa and isostatic cold pressing at 350 MPa. The disks, packed in SiC powder, were originally calcined in air (600 °C, 10 hrs.) and then sintered in nitrogen (1775 °C, 4 hrs). However, the calcining step was found to contribute to large non-uniform grain growth in the microstructure. Hence, the calcining step was omitted for the rest of the study.

As a comparison to the nanocomposite materials, pure Al_2O_3 specimens were also prepared in the same fashion, with the exception that the disks were packed in Al_2O_3 powder for the sintering process.

III. Experimental Procedure for Surface Residual Stress Study

The method used for determining the magnitude of macroscopic surface stress involved measurements of the elastic bending caused by the residual stress in thin plates [7]. Disk specimen were ground flat and polished down to 6 μm on one side. They were then attached to a rigid support and ground at 40 μm grid, 135N, and 150 r.p.m. on the other side until the sample thickness was reduced to $\approx$ 0.4 mm. Upon removal from the rigid support, the disks warped under the influence of the surface stresses introduced by grinding. The radius of curvature was measured using an optical interference setup (shown in Figure 1) and used to calculate the magnitude of surface residual stress. Subsequently, the same disk specimen was annealed at 1300 °C in argon for 2 hours, and the radius of curvature measured again.

IV. Result and Diskussion

An optical interference micrograph of a thin composite disk prepared in the manner described above is shown in Figure 2. A similar observation prior to the grinding step established that the initial curvature of the polished surface was negligible. Preliminary results indicate that grinding generates compressive surface stresses in the surface of the nanocomposites. When the disks were removed from the rigid support, the compression in the machined surface caused the disk to bend such that the polished surface became concave. If the surface stress were tensile, the polished surface would be convex. The determination of concavity was done by gently pressing on the center of the optical flat (referring back to Figure 1). For a concave curvature, the ring pattern should move toward the center, and vice versa for a convex curvature.

By counting the number of the rings corresponding to destructive interference (i.e., dark rings in Figure 2), the radius of curvature of the disk can be calculated using

$$R = r^2 / (n + 1/2)\lambda \qquad (1)$$

where R is the radius of curvature, r is the radius of the thin disk, n is the number of destructive rings, and λ is the wavelength of the laser illumination. The R value then allows the product of the average compressive stress, σ_R, and the thickness, t, of the compressive layer to be evaluated from the relation (for equibiaxial stress state)

$$\sigma_R t = Ed^2 / 6R (1 - \nu) \quad (2)$$

where d is the thickness of the disk ($d >> t$), E is the Young's modulus, and ν is Poisson's ratio [7]. Using E = 393 GPa and ν = 0.23, the average value of $\sigma_R t$ obtained for the grinding treatment was $\approx$ 1380 Nm^{-1}, which is consistent with previous measurement for machining damage in Al_2O_3 determined using the X-ray method [8].

Figure 3 is an optical interference micrograph of the same composite disk after annealing. The ring patterns have been replaced by curved lines. The disk is no longer concave but rather just warped unevenly. This result indicates that a significant proportion of the compressive surface stress have been relaxed. However, the stresses are not completely annealed out, which is in agreement with complementary studies by Fang et. al, namely, that surface machining stress in the nanocomposites are not relaxed completely by annealing in flowing argon at 1300 °C for 2 hours.

V. Conclusion

1. Grinding generates compressive surface stresses in the surface of the nanocomposites.

2. These surface stress do not relax completely during the annealing treatment used in this study.

The focus of future work will be a comparison of the surface residual stress behavior between pure alumina and nanocomposites, and testing of the effects of the surface stress upon the strength of the materials.

VI. References

[1] K. Niihara and A. Nakahira, Proceeding of the Third International Symposium on Ceramic Materials & Components for Engines, the American Ceramic Society, Westerville, OH (1988), pp. 919 - 926.

[2] K. Niihara, A. Nakahira, G. Sasaki, and M. Hirabayashi, Proceedings of the International Meeting on Advanced Materials, Vol. 4, the Materials Research Society, Japan (1989), pp. 124 - 134.

[3] K. Niihara, the Centennial Issue of the Ceramic Society of Japan, vo. 99, no 10, pp. 974 - 982 (1991).

[4] K. Niihara and A. Nakahira, Advanced Structural Inorganic Composites, edited by P. Vincenzini, Elsevier Sci. Pub. (1990), pp. 637 - 664.

[5] J. Zhao, L. C. Stearns, M. P. Harmer, H. M. Chan, G. A. Miller, and R. F. Cook, Journal of the American Ceramic Society, no. 2, (1993).

[6] L. C. Stearns, J. Zhao, and M. P. Harmer, Journal of European Ceramic Society, vo. 10, (1992), pp. 473 - 477

[7] D. Johnson-Walls, A. G. Evans, D. B. Marshall, and M. R. James, Journal of the American Ceramic Society, vo. 69, no. 1, (1986), pp. 44-46

[8] F. F. Lange, M. R. James, and D. J. Green, Journal of the American Ceramic Society, vo. 66, no. 2, (1983), pp. c-16 - c-17

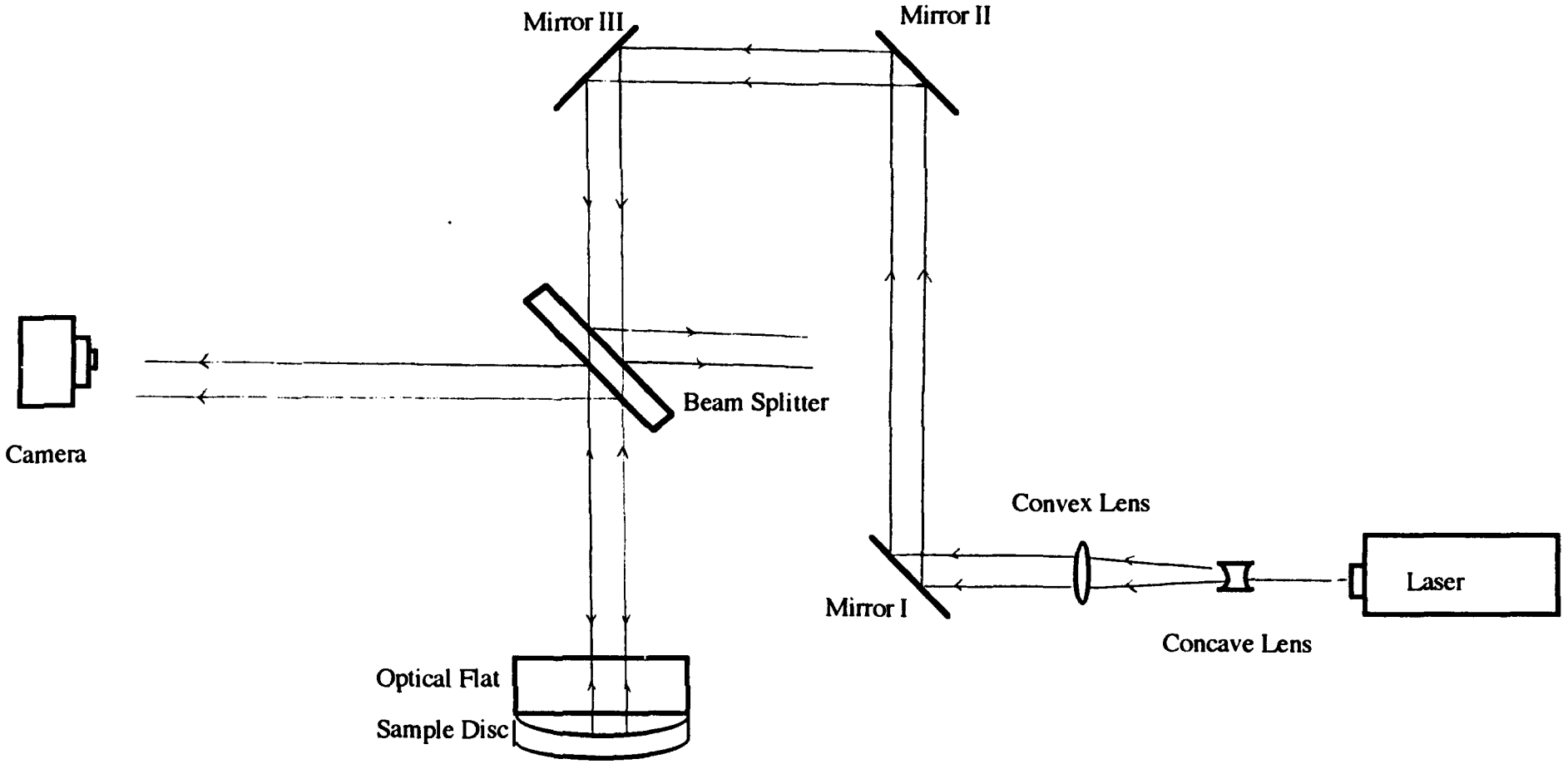

Figure 1. Laser Optical Interferometry Setup for Detection of Radius of Curvature

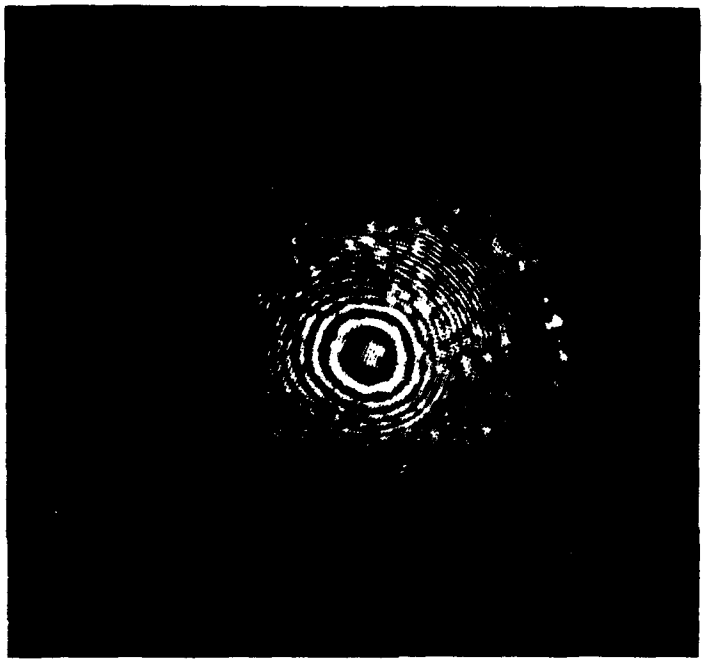

Figure 2. Optical interference micrograph of a thin composite disk after grinding treatment. The dark rings correspond to destructive interference. There are some minor interference distortion due to the small unevenness of the disk at the edge

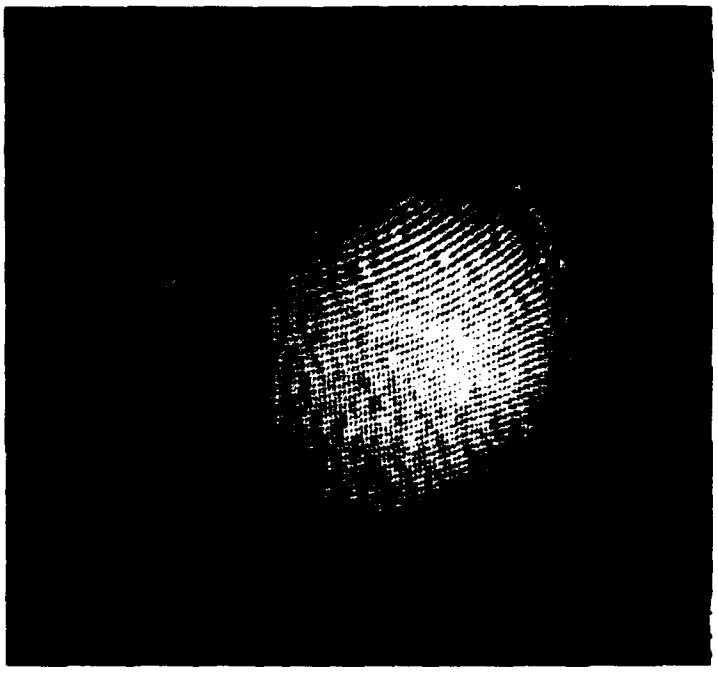

Figure 3. Optical interference micrograph of the same disk taken after annealing treatment at 1300°C for 2 hours in argon.

Section 2. Publications and Presentations

2. Publications and Presentations

H. M. Chan, M. P. Harmer, and G. A. Miller, "Application of Scanning Electron Microscopy to the Study of Multi-Phase Ceramic Composites", Proc. 51st Ann. Mtg. MSA, Eds., G. W. Bailey and C. L. Rieder, San Francisco Press, San Francisco, CA, 1993, pp. 946-47.

A. M. Thompson, H. M. Chan, M. P. Harmer, and R. F. Cook, "Crack Healing and Stress Relaxation in Al_2O_3SiC Nanocomposites", J. Am. Ceram. Soc. (Submitted).

A. M. Thompson, H. M. Chan, M. P. Harmer, and R. F. Cook, "'Flaw Healing' in Al_2O_3-SiC Nanocomposites", Ceramographic Exhibit at ACerS Annual Meeting, 1993 (appeared inside-back cover of J. Am. Ceram. Soc., August, 1993).

H. M. Chan, "Tailoring of Ceramic Microstructures for Improved Mechanical Properties", Ford, North Penn Electronics Facility, Lansdale, PA., February 26, 1993.

A. M. Thompson, J. C. Fang, I. A. Chou, H. M. Chan, and M. P. Harmer, "Fracture Behavior of Alumina Containing Sub-Micron SiC Particles", Annual Meeting of Am. Ceram. Soc., Cincinnati, OH, April 1993.

H. M. Chan, "Mechanical Behavior of Al_2O_3:SiC Nanocomposites", ONR Workshop on Novel and In-Situ Processing of Advanced Materials, NAS Study Center, Woods Hole, MA, June 2, 1993.

H. M. Chan, "Tailoring of Multi-Phase Ceramic Composites for Optimum Mechanical Properties", Meet 'N' 93 (First SES-ASME-ASCE Joint Mtg.), Univ. of Virginia, Charlottesville, VA, June 8, 1993.

H. M. Chan, "Application of SEM to the Study of Multi-Phase Ceramic Composites", 51st Ann. MSA Meeting, Cincinnati, OH, August 5, 1993.

A. M. Thompson, H. M. Chan, M. P. Harmer, and R. F. Cook, "Fracture Behavior of Alumina Containing Sub-micron SiC Particles", 1993 PAC RIM Meeting, Honolulu, HI, November 1993.

M. P. Harmer, "Microstructural Design of Multiphase Ceramic Composites for Optimum Mechanical Performance", Annual Meeting of the Brazilian Ceramic Society, Curitiba, Brazil, May 1993 (Invited).

M. P. Harmer, "Microstructural Design of Multiphase Ceramic Composites", Materials '93 Conference in Porto, Portugal, October 1993 (Invited).

M. P. Harmer, "Mechanical Behavior of Ceramics, University of Oporto, Portugal, October 1993.

Section 3. Awards and Accomplishments

3. Awards and Accomplishments

Martin P. Harmer elected Fellow of the American Ceramic Society, April 1993.

Third place ACerS Ceramographic Exhibit (SEM category) for poster entitled, "Machining Behavior of Al_2O_3-SiC 'Nanocomposite'", J. Fang, A. M. Thompson, H. M. Chan, and M. P. Harmer. (Appeared inside-back cover of J. Am. Ceram. Soc., July 1993).

Section 4. Personnel

4. PERSONNEL

Principal Investigator

Helen M. Chan

Co-Principal Investigator

Martin P. Harmer

Research Associates

A. Mark Thompson
J. C. Fang

Graduate Students

Irene A. Chou